Hydrol. Earth Syst. Sci., 20, 1765–1784, 2016
www.hydrol-earth-syst-sci.net/20/1765/2016/
doi:10.5194/hess-20-1765-2016

Hydrology and Earth System Sciences
Open Access
EGU

Investigating the impact of land-use land-cover change on Indian summer monsoon daily rainfall and temperature during 1951–2005 using a regional climate model

Subhadeep Halder[1], Subodh K. Saha[2], Paul A. Dirmeyer[1], Thomas N. Chase[3], and Bhupendra Nath Goswami[4]

[1]Center for Ocean–Land–Atmosphere Studies, George Mason University, Fairfax, VA 22030, USA
[2]Indian Institute of Tropical Meteorology, Dr. Homi Bhabha Road, Pashan, 411008 Pune, India
[3]Cooperative Institute for Research in Environmental Sciences (CIRES), Boulder, CO 80309, USA
[4]Indian Institute of Science Education and Research, Dr. Homi Bhabha Road, Pashan, 411008 Pune, India

Correspondence to: Subhadeep Halder (shalder3@gmu.edu)

Received: 27 April 2015 – Published in Hydrol. Earth Syst. Sci. Discuss.: 9 July 2015
Revised: 7 December 2015 – Accepted: 22 March 2016 – Published: 10 May 2016

Abstract. Daily moderate rainfall events, which constitute a major portion of seasonal summer monsoon rainfall over central India, have decreased significantly during the period 1951 through 2005. On the other hand, mean and extreme near-surface daily temperature during the monsoon season have increased by a maximum of 1–1.5 °C. Using simulations made with a high-resolution regional climate model (RegCM4) and prescribed land cover of years 1950 and 2005, it is demonstrated that part of the changes in moderate rainfall events and temperature have been caused by land-use/land-cover change (LULCC), which is mostly anthropogenic. Model simulations show that the increase in seasonal mean and extreme temperature over central India coincides with the region of decrease in forest and increase in crop cover. Our results also show that LULCC alone causes warming in the extremes of daily mean and maximum temperatures by a maximum of 1–1.2 °C, which is comparable with the observed increasing trend in the extremes. Decrease in forest cover and simultaneous increase in crops not only reduces the evapotranspiration over land and large-scale convective instability, but also contributes toward decrease in moisture convergence through reduced surface roughness. These factors act together in reducing significantly the moderate rainfall events and the amount of rainfall in that category over central India. Additionally, the model simulations are repeated by removing the warming trend in sea surface temperatures over the Indian Ocean. As a result, enhanced warming at the surface and greater decrease in moderate rainfall events over central India compared to the earlier set of simulations are noticed. Results from these additional experiments corroborate our initial findings and confirm the contribution of LULCC in the decrease in moderate rainfall events and increase in daily mean and extreme temperature over India. Therefore, this study demonstrates the important implications of LULCC over India during the monsoon season. Although, the regional climate model helps in better resolving land–atmosphere feedbacks over the Indian region, the inferences do depend on the fidelity of the model in capturing the features of Indian monsoon realistically. It is proposed that similar studies using a suite of climate models will further enrich our understanding about the role of LULCC in the Indian monsoon climate.

1 Introduction

Observational evidences show that globally averaged annual mean surface temperature has increased by about 0.85 °C between 1880 and 2012, with rapid warming in the recent past decades (about 0.72 °C after 1951) (IPCC AR5, Stocker et al., 2013). The number of cold (warm) days and nights have also decreased (increased) globally, with an increase in the frequency of heat waves over large parts of Europe, Asia, and Australia. There has also been an increase in extreme (heavy) precipitation events over most of the global land areas (Alexander et al., 2006; Stocker et al., 2013). According

to Allen and Ingram (2002), the increase in mean precipitation is expected to be much less than the extremes as it is constrained by the net rate of cooling of the troposphere, which in turn also depends on its temperature and presence of greenhouse gases (GHGs) and aerosols. On the contrary, Seneviratne et al. (2012) opined that there is no general relationship between changes in total and extreme precipitation. It is intriguing to note that seasonal and regional or local changes in extreme weather events can be of different magnitude and sign than global changes due to complex regional feedbacks associated with the GHGs, clouds, aerosols and other anthropogenic activities such as land-use/land-cover change (LULCC). For example, Haerter and Berg (2009) argue that changes in humidity, atmospheric stability, wind direction, etc., can strongly influence the local temperature variability. However, due to observational uncertainty, challenges in modeling and natural variability proper detection and attribution of the regional climate changes often becomes difficult. Therefore, quantification of the changes in regional climate as well as proper attribution are both very important.

1.1 Role of LULCC in climate

LULCC is an important driver of climate change at local, regional, and possibly, global scale (Snyder, 2010) and timescales inter-decadal and beyond (Pitman et al., 2012; Mahmood et al., 2014; Dirmeyer et al., 2010; Solomon et al., 2007). However, the climate effects of deforestation and agricultural intensification vary regionally and also depend on the seasons, making the resulting land–atmosphere interactions complex. In the last 300 years (1700–2000), about 42–68 % of the global land surface has been affected due to land use practices (Hurtt et al., 2006; Pielke Sr. et al., 2011), resulting in an increase in cropland (Ramankutty and Foley, 1999; Ramankutty et al., 2008) and pastures (Goldewijk, 2001). Robust results have shown that albedo changes due to an increase in croplands and pastures leading to a decrease in surface temperature tend to dominate over the mid-latitudes, whereas decrease in evapotranspiration (ET), roughness length, and cloudiness play a primary role in increasing surface warming in the tropics (Garratt, 1993; Bounoua et al. 2002; Feddema et al., 2005; Sampaio et al., 2007; Davin and De Noblet-Ducoudrè, 2010; Lawrence and Chase, 2010; Pitman et al., 2012). Furthermore, deforestation can affect moisture convergence, atmospheric stability, and changes in rainfall (Sud et al., 1998; Pielke Sr., 2001). Studies also suggest that changes in the temperature extremes due to LULCC could be of comparable magnitude but of similar or opposite sign due to increase in CO_2, depending on the region (Avila et al., 2012; Pitman et al., 2012). As it is difficult to segregate the impact of LULCC on temperature and precipitation extremes when analyzed in a globally averaged sense (Pielke Sr. et al., 2011; Pitman et al., 2012), carefully designed sensitivity studies with climate models focussing on specific regions are required.

1.2 Changes in temperature, rainfall, and LULCC over India

Observed changes in daily temperature and rainfall extreme events over the Indian region may be attributed to both natural variability and anthropogenic activity. There has been an increase of about 0.5 °C in the annual mean and 0.71 °C in the maximum temperature over India in the last century, but increased warming in the recent decades (1971–2003) (Kothawale and Rupa Kumar, 2005; Kothawale et al., 2010). Pai et al. (2013) noted a significant increase in the occurrence of heat waves in summer (1961–2010), whereas Jaswal et al. (2015) showed an increase in temperature extremes (1969–2013). Observed changes in temperature in recent decades have been associated with the effect of increasing aerosols (Pai et al., 2013; Sheikh et al., 2014), as reported earlier by Krishnan and Ramanathan (2002). Over central India (CI; 74.5–86.5° E, 16.5–26.5° N), daily heavy and very heavy rainfall events during the monsoon season (June–September, JJAS) have shown significant increasing trend during 1951 to 2000, whereas moderate rainfall events have shown significant decreasing trend (Goswami et al., 2006; Rajeevan et al., 2008; Pai and Sridhar, 2015). Above studies proposed that significant warming of sea surface temperatures (SSTs) over the equatorial Indian Ocean in recent decades could be a plausible reason for the increase in precipitation extremes, however the mechanism for changes in moderate rainfall events remains unexplored. There has also been an increase in the intensity of droughts over India during 1901 to 2010 (Niranjan Kumar et al., 2013) and a significant decrease in wet days and moderate and total rainfall during the summer monsoon (1971–2005) (Panda and Kumar, 2014). Both studies have associated the observed changes to variations in SST over the Indian and Pacific oceans. Furthermore, rapid warming of the Indian Ocean compared to land has been shown to have significantly affected the land–sea thermal contrast and decreased summer rainfall during 1901–2012 (Roxy et al., 2015). Apart from regional changes in the concentration of anthropogenic aerosols and GHGs or the Indian Ocean SSTs, industrialization and urbanization over India have lead to widespread deforestation and changes in land-use practices in recent decades. According to Tian et al. (2014), there has been a loss of about 26 million ha of forests and gain of about 48.1 million ha of crops in India during 1880–2010 (cf. Fig. 4 in their paper). Therefore, the impact of LULCC alone on changes in the distribution of moderate rainfall events or surface temperature extremes during 1951–2000 needs to be investigated.

Studies have attempted to understand the mechanisms through which LULCC affects the regional climate over India. For example, Sen Roy et al. (2007,2011) demonstrated that irrigation can lead to a significant decrease (increase) in pre-monsoon surface temperature (precipitation) over India. Irrigation activity has also been shown to affect the Indian Summer Monsoon Rainfall (ISMR) through changes in

land-ocean temperature contrast (Lee et al., 2009) or land–atmosphere feedbacks (Niyogi et al., 2010; Tuinenburg et al., 2011). There have been several other studies addressing the effects of LULCC over the Indian region (Lohar and Pal, 1995; Douglas et al., 2006, 2009; Niyogi et al., 2007; Saeed et al., 2009; Dutta et al., 2009; Nayak and Mandal, 2012). Apart from them, Lei et al. (2008), Kishtawal et al. (2009), and Ali et al. (2014) explored the impact of growing urbanization in India and large-scale climate variability in the changes in extreme rainfall events. Interesting time slice experiments made with a global model have shown that an increase in crop and pasture land lead to a decrease in seasonal rainfall over India during the pre-industrial period (years 1700–1850) when the impact of anthropogenic activity or natural climate variations were minimal (Takata et al., 2009). Krishnan et al. (2015) made several experiments with a high-resolution global atmospheric model and concluded that a multitude of factors such as aerosols, land-use change, Indian Ocean warming, as well as GHGs, have together contributed to the observed weakening of the south-Asian monsoon and changes in frequency distribution of daily rainfall events during the later half of the 20th century. However, the impact of LULCC as a lone forcing component on the Indian summer monsoon has not been quantified. It is also plausible that feedbacks due to variations in remote SSTs and snow cover may have modulated the local impacts due to LULCC. In this study, we hypothesize and demonstrate that LULCC has partly contributed to the observed decrease in moderate rainfall events over CI during the monsoon season from 1951 to 2005, apart from the increasing trend in daily mean and maximum temperatures. We have conducted experiments with a high-resolution regional climate model (RCM) RegCM4.0 and much improved and up-to-date land cover data over the Indian region to prove our hypothesis. No added external forcing in terms of aerosols or GHG concentrations is used in our experiments. Furthermore, additional experiments by removing the positive trend in Indian Ocean SSTs have also been made to isolate the impact of LULCC.

RCMs have shown much improvement over global climate models (GCMs) in terms of representation of spatiotemporal details of climate (Giorgi and Mearns, 1999; Laprise et al., 2008; Leduc and Laprise, 2009) and dynamical downscaling ability (Xue et al., 2014), and added value in simulation of topography induced phenomena and extremes of short spatiotemporal character (Feser et al., 2011; Feser and Barcikowska, 2012; Shkol'nik et al., 2012). Saha et al. (2011, 2012) and Halder et al. (2015) made experiments with the RCM RegCM3 and RegCM4, respectively, to better resolve regional land–atmosphere feedback processes and demonstrate their role in the mean and variability of the Indian summer monsoon. When time-dependent lateral boundary conditions are used as forcing for a RCM in one-way mode, feedback from the model-simulated climate to the global climate is not allowed. Interactions between large-scale forcing such as El Niño–Southern Oscillation (ENSO) that is external to the Indian monsoon region and internal monsoon dynamics may lead to more variability than due to local feedback processes. Therefore, our methodology helps in segregation of the impact of regional LULCC on the Indian summer monsoon and its changes. However, one of the drawbacks of regional climate modeling is that lateral boundary conditions are not perfect. Our paper is organized in the following way. Observed data, the RCM and the design of experiments are described in detail Sect. 2. The method of preparation of the land cover data used for model experiments is described in the supplementary material. The observed changes in near-surface temperature and rainfall and LULCC over the Indian subcontinent in the last 55 years are discussed in Sect. 3. Results from model experiments pertaining to changes in rainfall and surface temperature are discussed in detail in Sect. 4. Discussions are presented in Sect. 5 and the conclusions drawn are summarized in Sect. 6.

2 Data and methods

2.1 Observed data

Daily 2 m mean and maximum temperature data (1969–2005; at $1^\circ \times 1^\circ$ resolution) from the India Meteorological Department (IMD) (Srivastava et al., 2009) are used for analysis of trends and validation of the model simulations. In addition to that, we have also used daily 2 m mean temperature data (at $2.0^\circ \times 2.0^\circ$ resolution) of the twentieth century reanalysis (20CR) project (Compo et al., 2011) that is available for a longer period (1951–2005). For analysis of trends in daily rainfall events and their intensities in different categories daily gridded data for 55 years (1951–2005) from the Asian Precipitation Highly Resolved Observational Data Integration Towards Evaluation of Water Resources (APHRODITE Water Resources; Yatagai et al., 2012) at $0.5^\circ \times 0.5^\circ$ resolution is used. Monthly rainfall from Global Precipitation Climatology Project (GPCP) version 2.2 (Adler et al., 2003) for the period 1982–2008 (at $2.5^\circ \times 2.5^\circ$ resolution) is also used for validation of model simulated rainfall. Apart from that, the National Centers for Environmental Prediction/National Center for Atmospheric Research (NCEP/NCAR) monthly reanalysis winds, temperature, and specific humidity (Kalnay et al., 1996) for the period 1982–2007, at $2.5^\circ \times 2.5^\circ$ horizontal resolution and multiple pressure levels are used for validation of the model simulated large-scale features during monsoon.

2.2 Land cover data

Annual harmonized land cover data (LUHa.v1) from the University of New Hampshire (UNH; http://luh.unh.edu) at $0.5^\circ \times 0.5^\circ$ horizontal resolution (Hurtt et al., 2006) that is comprised of crop, pasture, and primary and secondary vegetation types has been used in this study. This data have been transformed in the form of 17 plant functional type (PFT)

mosaics for use as a time invariant lower boundary condition for simulations with the RCM. The four UNH vegetation categories are converted into different PFT distributions based on present-day and potential vegetation for community land model (CLM) land-surface parameters. We have used the resulting PFT distributions and associated vegetation-dependent parameters such as leaf area index (LAI), stem area index (SAI), roughness length, etc., for the present-day conditions (year 2005) and historical period (year 1950) for our model simulations. Detailed methodology of preparation of the land cover data are given in the Supplement.

2.3 RegCM4.0 and the CLM3.5 land-surface model

The RCM RegCM4.0 (Elguindi et al., 2010; Giorgi et al., 2012) is used for this study. The dynamical core of RegCM4 is from the NCAR – Pennsylvania State University (PSU) Mesoscale Model version 4 (MM4), which is a compressible, finite difference model with hydrostatic balance and vertical σ coordinates. The NCAR CCM3 radiation scheme (Kiehl et al., 1996) and a planetary boundary layer scheme based on a non-local diffusion concept (Holtslag et al., 1999) are used for our simulations. We have also used the parameterization scheme of Zeng and Beljaars (2005) that allows for a realistic representation of the diurnal variation of sea surface skin temperature. Apart from that, the Grell convective parameterization scheme (Grell, 1993) with the Fritsch and Chappell closure (Fritsch and Chappel, 1980) is used. The model configuration is comprised of 23 vertical sigma coordinate levels in the atmosphere and a horizontal resolution of $60^\circ \times 60^\circ$ with normal Mercator map projection. The model domain extends from 40.2 to 116.3° E and 10.8° S to 47.7° N with the Indian subcontinent at the center. The NCEP/NCAR reanalysis data (Kalnay et al., 1996) at $2.5^\circ \times 2.5^\circ$ horizontal resolution and 6-hourly frequency for the period 1982 to 2008 is used as lateral boundary conditions for the model. Reynolds weekly SST at $1^\circ \times 1^\circ$ horizontal resolution (Reynolds et al., 2002) interpolated to daily values is prescribed over the ocean.

RegCM4.0 is coupled to the CLM3.5 (Oleson et al., 2008; Stockli et al., 2008) land-surface model. There are 10 soil layers of variable depth and up to 5 layers of snow. CLM3.5 uses a nested sub-grid hierarchy of mosaics in the form of glaciers, lakes, wetlands, urban, and vegetated land to better represent surface heterogeneity in a grid box. The vegetated land portion of a grid cell may be composed of multiple columns. Furthermore, in each column the four most abundant PFTs out of possible 17 that include forests, grasses, crops, and bare ground co-exist. The fractional areas of the four PFTs do not vary with time but their leaf and stem area indices vary seasonally, which are all interpolated from global data sets at $0.5^\circ \times 0.5^\circ$ horizontal resolution to the model grid. Fluxes are computed at the PFT level and their weighted averages constitute the net upward flux from a column. Several PFT-based parameters are also prescribed in the model. The GTOPO30 topography data at 30 arcsec resolution courtesy of the USGS (United States Geological Survey) Earth Resources Observation Systems (EROS) Data Center has been used in this study. A global soil texture data set at 5 min spatial resolution from the International Geosphere Biosphere Program (IGBP) (Bonan et al., 2002) is used with varying sand and clay content in each of the 10 layers. Soil color data set (eight classes) at 2.8×2.8 spatial resolution is from Zeng et al. (2002). CLM3.5 also uses global data sets on canopy top and bottom height (resolution 0.5×0.5), percentage of glacier (resolution 0.5×0.5), lake and wetland (resolution 1×1) with corresponding spatial resolution included in brackets (Elguindi et al., 2010). Details about the parameterization schemes in CLM3.5 are also presented in Oleson et al. (2010) and Halder et al. (2015).

2.4 Design of experiments and methodology

Two sets of model simulations, each for 27 years are carried out with similar lateral boundary conditions (LBCs) from NCEP/NCAR reanalysis and Reynolds weekly SST prescribed at the lower boundary, but different land cover for the years 1950 and 2005 as fixed lower boundary condition. The land cover of 1950 and 2005 correspond to different PFT distributions. The RCM is initialized at 00:00 GMT on 1 November 1981 and the simulation is continued up to 18:00 GMT on 31 December 2008. In CLM3.5 coupled to RegCM4, soil moisture is initialized based on climatological values (as in Giorgi and Bates, 1989; Halder et al., 2015), in order to reduce model spin-up time for the deeper soil layers. Therefore, we have discarded the initial 7 months for model spin up. Soil points are initialized with temperatures of 283 K (Oleson et al., 2010). Hereafter, these simulations with land cover of 2005 and 1950 will be referred as present land cover (PLC) and historical land cover (HLC) experiment, respectively. Studies have suggested that changes in surface temperature (Kothawale et al., 2010; Chowdary et al., 2013) and extreme rainfall events (Krishnan et al., 2015) over India are related with variations in the Indian Ocean SSTs. Therefore, in order to isolate the effect of Indian Ocean SSTs on the temperature and rainfall variability over the Indian region, another pair of model simulation for the same 27 years are carried out using the fixed land cover of years 1950 and 2005, but with de-trended Reynolds SSTs over the Indian Ocean. The LBCs from NCEP/NCAR reanalysis and the initial conditions remained exactly same as in the earlier experiments. Henceforth, these RCM simulations will be referred as present land cover de-trended SST (PLCS) experiment and historical land cover de-trended SST (HLCS) experiment, respectively. The four experiments are briefly summarized in Table 1.

Our objective is to analyze changes in the climatological mean of the number of moderate rainfall events over CI and intensity of rainfall in that category, between PLC and HLC experiments. The lateral boundary forcing and prescribed

Table 1. Experimental setup for LULCC-based simulations with RegCM4.

Experiment name	Lateral boundary conditions	Sea surface temperature	Year of fixed land cover	Period of simulation
PLC	1 Nov 1981–31 Dec 2008	Observed (1981–2008)	2005	27 years
HLC	1 Nov 1981–31 Dec 2008	Observed (1981–2008)	1950	27 years
PLCS	1 Nov 1981–31 Dec 2008	De-trended (1981–2008)	2005	27 years
HLCS	1 Nov 1981–31 Dec 2008	De-trended (1981–2008)	1950	27 years

SST in our experiments are transient in nature and impose the global warming signal on the model climate. As each year of forcing is different from the other, long-term mean is expected to be closer to the reality. However, use of climatological boundary conditions is not an option, as in that case the model will have a problem properly capturing the synoptic and intraseasonal rainfall variability that contribute to the seasonal mean rainfall significantly. Similarly, a single year (ENSO/non-ENSO year) of boundary condition cannot be repeated as that may lead to biased response of the model climate to LULCC. As time varying lateral boundary conditions also impose the effect of variations in remote SSTs, such as that of the Pacific Ocean on the model, partial remote influence on the nature of response due to regional LULCC is possible. Although our RCM simulations are not time-slice experiments in the true sense, the statistics of their difference are expected to reveal the effect of LULCC and associated regional land–atmosphere feedbacks on daily temperature and rainfall variability in a climatological sense.

Extreme rainfall events are short lived, less frequent, but intense. They are associated with deep convective activity that is triggered by local instabilities or large-scale moisture convergence and drain out the atmospheric moisture content very fast, thus increasing the atmospheric stability. On the other hand, light and moderate rainfall events are relatively less intense and long lived and require time for large-scale moisture and instability to build up and be sustained. Thus, due to the smaller spatial scale and random frequency of occurrence of extreme rainfall events, analysis of their trends over stations sparsely spaced or individual grid points is not expected to give a robust or consistent result about their temporal variability. However, more meaningful information on the statistics of extreme rainfall events can be obtained when analyzed in a spatially aggregated sense (Goswami et al., 2006; Rajeevan et al., 2008; Singh et al., 2014). For our study, the CI domain that is considered homogeneous in terms of the mean and variability of the Indian summer monsoon rainfall (Goswami et al., 2006) is used for the analysis of moderate and extreme rainfall events. Significance of the results have been tested on the basis of Student's *t* test. For the analysis on temperature extremes in the model we have used data for the period JJAS (instead of JAS used for observation) that will be further discussed in Sect. 4.1.

3 Observed changes

3.1 LULCC

Figure 1 shows the distribution of PFTs in the year 1950 and 2005 used as lower boundary condition in the RCM and also gives an overview of past changes in land cover. The northwest of India, the hilly terrain over CI, western states of Gujarat and Maharashtra, foothills of the Himalayas, and northeastern states are mostly dominated by forest cover (Fig. 1a and c). Agriculture or crop cover is mostly concentrated along the northern states of India such as Punjab, Haryana, Delhi, the Gangetic plains, the plains of eastern and western CI, and peninsular India (Fig. 1b and d). Difference between PFT distribution under the present climatic conditions (year 2005) and the historical period (year 1950) show that forest cover is reduced and crop cover is increased in the recent period by about 5–30 % (Fig. 1e and f). Maximum increase in crop fraction is seen largely over CI, peninsular India, north and northwest of India, and the extreme northern part around the plains of river Indus. This increase in crop fraction also matches very well with the changes shown in Fig. 5 in the study by Tian et al. (2014) over the period from 1950 to 2010. It is interesting to note that observed surface evaporation has significantly decreased over continental India during the monsoon season from 1971 to 2000 (Jaswal et al., 2008), which may have been associated with the LULCC.

3.2 Rainfall over central India

There is no clear trend in the India mean summer monsoon rainfall during JJAS from 1951 to 2000, but extreme and moderate rainfall events have changed over CI significantly. Following Goswami et al. (2006) and Rajeevan et al. (2008), moderate rainfall events are defined in this study as $5 > \text{rainfall} \leq 100\,\text{mm day}^{-1}$, whereas heavy and very heavy rainfall events are defined as $\text{rainfall} \geq 100\,\text{mm day}^{-1}$ and $\text{rainfall} > 150\,\text{mm day}^{-1}$, respectively. After counting daily rainfall at each grid point over CI as an event during JJAS from 1951 to 2005 and fitting a linear trend, we find that the number of moderate rainfall events in these 55 years have significantly decreased by about 640 (which is about 3 % of the initial value in 1951) (Fig. 2a). Associated with that, total rainfall in the moderate category has also decreased during

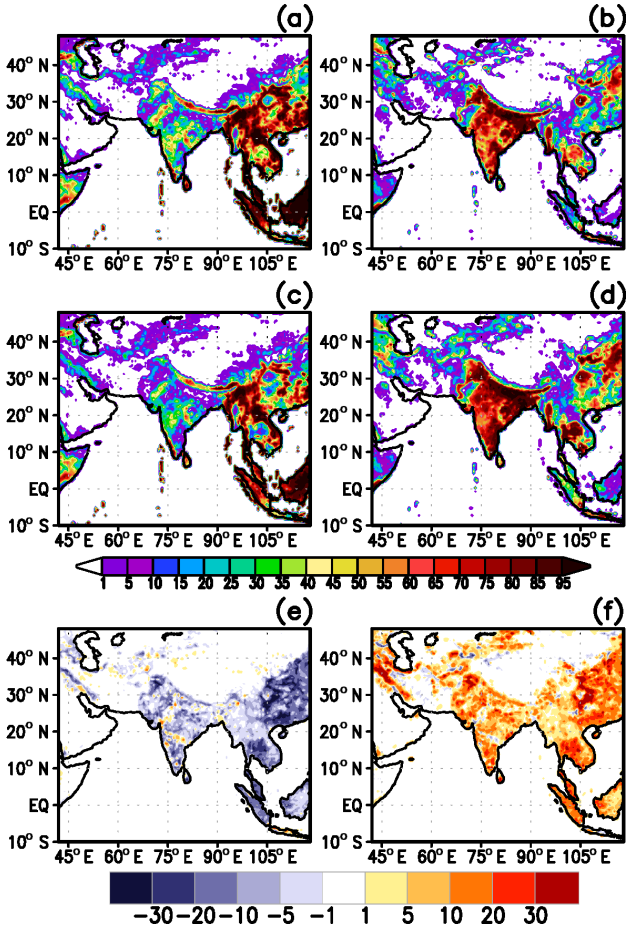

Figure 1. PFT distribution of forest and crop cover (in %) used as fixed lower boundary condition in the model experiments. **(a)** Forest and **(b)** crop of the year 1950 (HLC). **(c)** Forest and **(d)** crop of the year 2005 (PLC). Differences (PLC–HLC) in **(e)** forest and **(f)** crop cover.

JJAS (Fig. 2b). The number of extreme rainfall events over CI has significantly increased by eight (almost double the value in 1951) between 1951 and 2005 (figure not shown). We propose that LULCC during these 55 years might have contributed to the observed decrease in moderate rainfall over CI and substantiate our hypothesis using multiple simulations with the RCM RegCM4.

3.3 Surface air temperature

The pre-monsoon season in India (March–April–May) is characterized by days that are hot and dry. The climatological onset date of the southwestern monsoon over Kerala (southern tip of India) is 1 June. There is large year-to-year variability in the date of onset and in many years, onset takes place during the middle of June (Wang et al., 2009). Therefore, to investigate the changes in observed daily mean temperature and its extreme during the monsoon season, trends are calculated using temperature of the months July–September (JAS)

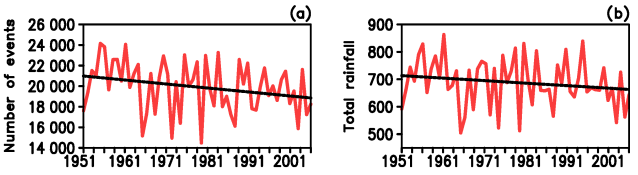

Figure 2. Time series of number of observed moderate rainfall events over CI and total rainfall in JJAS (in mm; 1951–2007) from APHRODITE rainfall data. **(a)** Moderate rainfall events and **(b)** total amount of rainfall in moderate category. Black dotted line represents the linear trend.

only. A warming trend in the JAS mean temperature by 0.2–0.4 °C decade^{-1} is observed over the northwest, northeast, and southern parts of India (Fig. 3a). Similar to the mean, extreme of daily mean temperature in JAS (its 90th percentile) also shows a warming trend, but over a larger region (Fig. 3b). Based on this trend from 1969 to 2005, it is estimated that the daily mean surface temperature and its extreme in JAS have increased by a maximum amount of about 1.11–1.48 °C. We have also analyzed the maximum temperature attained during the day, that represents the higher extreme. Figure 3c shows the trend in JAS-averaged daily maximum temperature. It is evident that warming in the daily maximum temperature is of the same order, but is more widespread as compared to the daily mean and includes areas north of CI. Furthermore, the 90th percentile of daily maximum temperature has increased by more than 1.48 °C over north-central India, which is greater than the increase in the mean (Fig. 3d). It may be noted that the spatial pattern of increase in daily temperature over CI is consistent with the area of increase in crop PFTs over CI and northwest (Fig. 1f). Similarly, the decreasing trend in daily temperature over areas south of CI also coincides well with the small increase in forest cover over that region (Fig. 1e). Increased observed temperature over the western coast of peninsular India may have happened due to its region specific mean climate predominantly determined by the adjoining Arabian Sea and Indian Ocean.

Trends in daily 20CR 2 m mean temperature data and its extreme (90th percentile) during JAS are further analyzed for the extended period 1951–2005. A significantly increasing trend is evident both in the mean and its extreme, over northern India (Fig. 3e), north of CI (Fig. 3f), and southern parts of peninsular India. The maximum increase in daily mean temperature in JAS is about 1.11 °C. The pattern of increase in daily maximum temperature is not only more widespread (possibly due to coarser resolution of the data) but also its magnitude is also comparable to that seen over the 37-year period (1969–2005). Apart from that, a decrease south of CI and an increase towards the extreme south is also evident. However, while comparing the trends shown by the above two data sets we note that the model used to generate the 20CR data did not assimilate surface temperature observa-

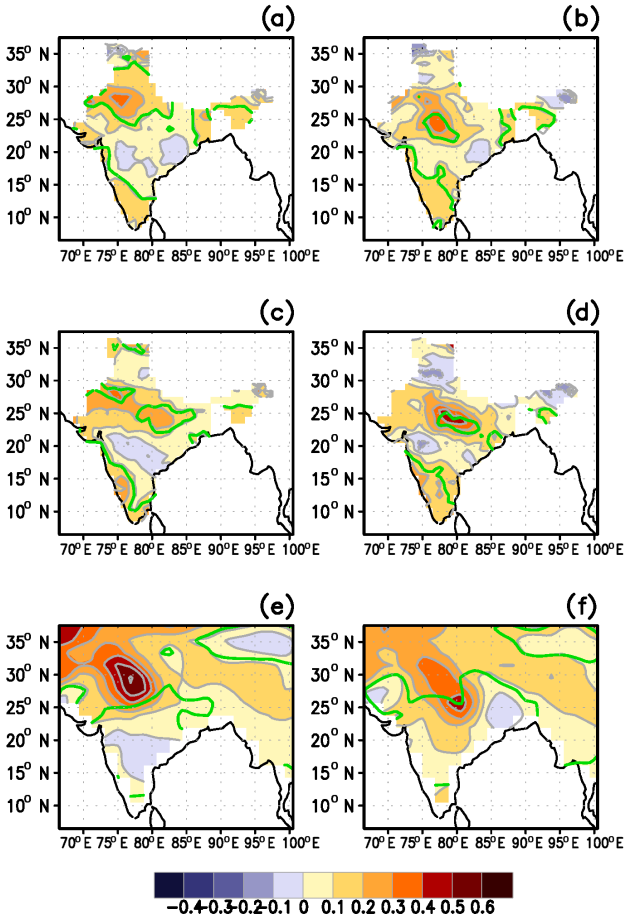

Figure 3. Observed trend (1969–2005) in seasonal (JAS) 2 m air temperature from IMD (in °C decade^{-1}). Trend in **(a)** seasonal average of daily mean, **(b)** 90th percentile of daily mean, **(c)** seasonal average of daily maximum, and **(d)** 90th percentile of daily maximum temperature. Observed trend (1951–2005) in **(e)** seasonal average of daily mean and **(f)** 90th percentile of daily mean 2 m air temperature from 20CR reanalysis data (in °C decade^{-1}). Green contour encloses the region where trends are significant at the 90 % confidence level.

tions. Therefore, the resulting trend is also partially model dependent. The observed increasing trend in daily mean surface temperature and its higher extreme may be attributed to forcing of natural origin (solar, volcanic), anthropogenic origin (GHGs, aerosols, LULCC, etc.), or both. We aim to quantify the contribution of such an increase due to LULCC over India.

4 Results from RCM experiments

In the PLC and HLC experiments, we keep the atmospheric and oceanic boundary conditions during 1982 to 2008 same but the distribution of PFTs are altered corresponding to years 2005 and 1950, respectively. This experimental setup is meant to help us understand the statistics of changes in rainfall and temperature due to LULCC.

4.1 Indian summer monsoon features in PLC and PLCS experiments

The skill of the RCM in capturing the mean spatial distribution of seasonal (JJAS) rainfall and its interannual variability are assessed here. The observed seasonal mean monsoon rainfall in GPCP (Fig. 4a) shows a region of maxima over the western Ghats, head Bay of Bengal (BoB), hilly terrain of central India, and northeastern India. There is also a region of maximum over eastern equatorial Indian Ocean. In comparison, rainfall in the PLC experiment is overestimated near the Arabian Sea coast and over BoB. Apart from that, a secondary rainfall maximum that is shifted to the western equatorial Indian Ocean region is also noted in PLC. Although rainfall is captured over CI and the northeastern region, the magnitude appears to be underestimated, particularly over western India. Studies have shown that the rainfall bias in this RCM over the ocean is attributed to the lack of coupling with the atmosphere and also to the choice of convective parameterization schemes (Chow et al., 2006; Ratnam et al., 2009; Saha et al., 2011; Halder et al., 2015). However, it is interesting to note that compared to an earlier version of the RCM (RegCM3) used for simulation of the Indian summer monsoon with a similar model setup (Saha et al., 2011, 2012), this positive bias over the western equatorial Indian Ocean region and western part of BoB is relatively reduced. The dashed (solid) lines in Fig. 4b represent the CI (big-India, BI) domain used for our analysis related to the statistics of daily rainfall. Seasonal mean rainfall in the PLCS experiment follows a similar spatial pattern as in the PLC and captures the locations of rainfall maxima very well (Fig. 4c). However, the magnitude is relatively less everywhere compared to the PLC experiment. Maximum decrease in seasonal total rainfall over CI between the PLCS and PLC experiments is about 4 cm (figure not shown). This decrease is possibly associated with relatively colder SSTs over the Indian Ocean that leads to lesser evaporation over the ocean and hence moisture in the atmosphere. These aspects will be discussed further in Sect. 4.2.

Seasonal rainfall over the land part in PLC (Fig. 4e) is further compared in detail with that from APHRODITE data (Fig. 4d). The representation of orography in the model is depicted in Fig. 4f, which suggests that the surface topography is very well captured by the model. It is evident that the RCM reproduces the regions of rainfall maxima and the spatial pattern very well, particularly over the western Ghats section over peninsular India, CI, northeastern India, and the Himalayan foothills. The rain-shadow area east of the western Ghats is also captured very well by the RCM. However, it slightly underestimates the magnitude of rainfall over the peninsular and western part of India (also reported in

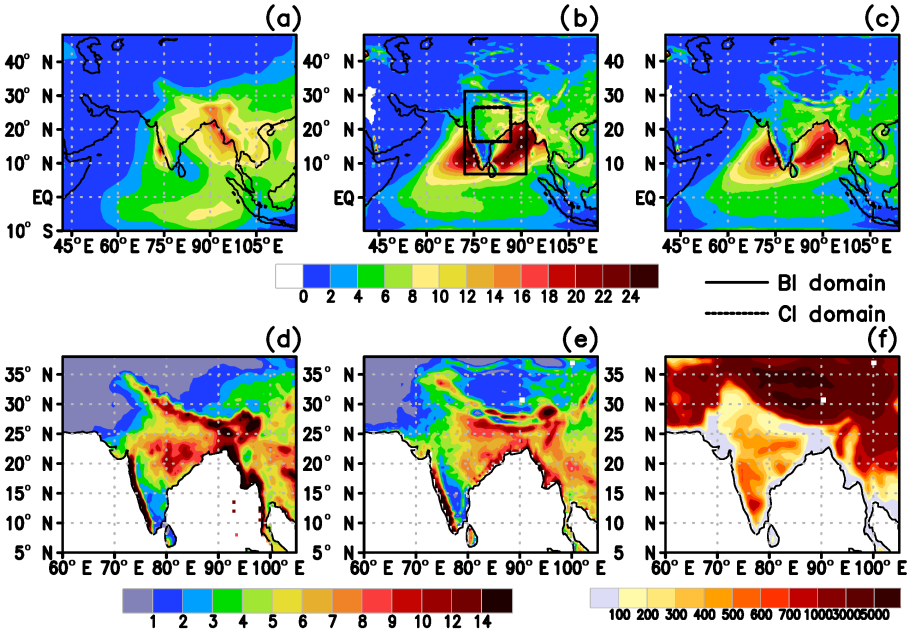

Figure 4. Seasonal (JJAS)-averaged rainfall **(a)** from GPCP (1982–2008), **(b)** in PLC experiment (1982–2008), **(c)** in PLCS experiment (1982–2008), and **(d)** based on APHRODITE data (1982–2007). **(e)** Seasonal-averaged rainfall only over land in PLC experiment. Units are in mm day^{-1}. **(f)** Representation of orography in RegCM4. Units are in m.

Halder et al., 2015). The pattern correlation between rainfall in the PLC experiment and APHRODITE is 0.71. The mean bias calculated over the presented domain with respect to APHRODITE rainfall for the period 1982–2007 is -0.48 mm day^{-1} and the RMSE is 3.53 mm day^{-1}. Although daily CI-averaged rainfall during JJAS in both observation and the PLC experiment (CI domain for the RCM is 75.30–86.63° E, 16.92–26.43° N) follows the Poisson distribution, the number of very heavy rainfall events simulated in the RCM is relatively less (figure not shown). This deficiency in climate models in terms of capturing the observed frequency distribution of daily rainfall realistically is a well-known problem (Frei et al., 2003; Kang et al., 2014) and may be attributed to the model dynamics, choice of convective parameterization schemes and their interplay (Frei et al., 2003). The mean and interannual standard deviation of CI-averaged rainfall (1982–2007) in PLC (APHRODITE) are 77.59 cm (87.28 cm) and 7.57 cm (8.8 cm), respectively. Therefore, the model performs well in capturing the observed interannual variability of seasonal rainfall over CI (which is about 10 % of the seasonal mean), although it underestimates both quantities.

We further evaluate JJAS-averaged 2 m near-surface air temperature simulated by the model with the IMD data for the period 1982–2005. Mean surface temperature in observation in highest over the northern, northwestern, eastern, and the rain-shadow region over the peninsular India (Fig. S1a in the Supplement). In contrast, surface temperature simulated by the model is high particularly over the northwest

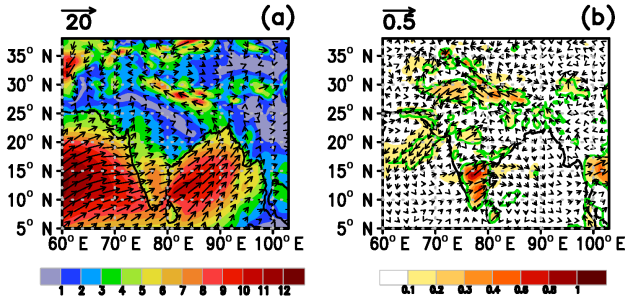

Figure 5. Seasonal (JJAS)-averaged wind at 10 m (in m s^{-1}; 1982–2008). **(a)** Climatological mean (PLC experiment) and **(b)** difference (PLC–HLC). The shaded color depicts magnitude and arrows show the direction. Green contour shows differences significant at the 90 % confidence level.

(Fig. S1b). A cold bias of about 3–4 °C in temperature is found over the rest of the Indian region that is linked with biases in the land surface as well as other parameterization schemes in the model such as radiation, convection, etc. (Fig. S1c). Such biases have also been noted and discussed in Halder et al., (2015). The pattern correlation between IMD and RegCM4 simulated JJAS 2 m air temperature is 0.76. A similar pattern of cold bias in 2 m near-surface air temperature is also seen in the PLCS experiment (figure not shown). As our objective is to analyze the mean differences between model simulations, these biases are not expected to have significant effect on the results.

Observed large-scale circulation features from the NCEP/NCAR reanalysis in the lower troposphere (850 hPa) shows the location of the low-level Somali jet over the Arabian Sea, cross-equatorial flow, and the easterlies south of the Equator (Fig. S2a). The RCM captures the location of these large-scale low-level features very well in both PLC and PLCS (Fig. S2b and c). However, the wind speed is slightly overestimated in the PLC experiment, particularly along the core of the Somali jet and the BoB. As mentioned earlier, this overestimation conforms to the positive rainfall bias over the ocean, the Arabian Sea, and the BoB in the RCM. On the contrary, low-level wind speed is reduced around the core of the jet, over the Indian Ocean, BoB, and also over land in the PLCS experiment, which is associated with the reduction in precipitation. At 200 hPa, observed circulation shows the sub-tropical westerly jet stream about north of 30° N, the tropical easterly jet over the equatorial Indian Ocean and the Tibetan anticyclone south of 30° N (Fig. S2d). The location of these characteristic circulation features is also well captured in the simulations PLC and PLCS (Fig. S2e and f). The model simulated wind speed is stronger than observations in the PLC experiment at upper level like at 850 hPa. The pattern correlation between NCEP/NCAR reanalysis and PLC simulated wind at 850 hPa (200 hPa) is 0.81 (0.95). We infer that the model RegCM4 performs well in simulating the climatological mean features of Indian summer monsoon. This gives us confidence to conduct sensitivity experiments with the model.

The climatological onset date of ISMR based on the tropospheric temperature gradient (TTG) index (Xavier et al., 2007) in the PLC experiment is around 20 May, with interannual standard deviation of about 8 days. Hence, it is advanced by about 10 days from the observed onset. Unlike in the observations, ISMR onset in the model happens to be in the month of May for most years. Therefore, for our analysis of temperature extremes in the model we have used data for the period JJAS (instead of JAS) in order have a longer time series and more confidence in the model results.

4.2 Changes in circulation and seasonal rainfall due to LULCC

Mean surface winds (at 10 m) during JJAS blow from west to east over peninsular India and the Indian Ocean, carrying moisture from the Arabian Sea. They turn counterclockwise over the BOB to move northwest over the Gangetic plains, thus forming the monsoon trough all along CI where the mean wind speed is very low (Fig. 5a). As forest cover in the HLC experiment is replaced by crop PFTs over most of the land part in the PLC experiment, surface roughness length is decreased due to reduction in vegetation height and LAI. We note that surface wind has become more westerly (easterly) over southern and western (northern) India in PLC than HLC and shows increased cyclonic circulation (Fig. 5b). It has intensified significantly by about 1 m s^{-1} over peninsular India

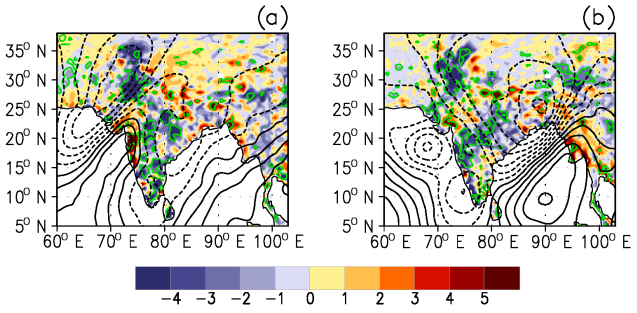

Figure 6. (a) Difference (PLC–HLC experiment) in climatological mean seasonal rainfall (in cm; 1982–2008) shown in shaded color. **(b)** Same as in **(a)** but for PLCS–HLCS experiments. Dashed (solid) black contours show the decrease (increase) in velocity potential analog (or the divergent component) of vertically integrated moisture flux $q\,\boldsymbol{V}$ (from surface–300 hPa). The contour interval is in 1×10^6 kg s^{-1}. Green contour shows differences significant at the 90 % confidence level.

and 0.5 m s^{-1} over the northern India (Fig. 5c). This implies less convergence of moisture and also a reduction in rainfall in the PLC experiment (see Sud et al., 1998; Takata et al., 2009) that is discussed in the following paragraph. This intensification of surface wind speed further extends up to the depth of the boundary layer that interacts more directly with the large-scale circulation (figure not shown). Surface and boundary layer winds also intensify in a similar fashion in the PLCS experiment when compared to HLCS and depict the effect of reduced roughness length due to LULCC. It is interesting to note that these significant changes take place mainly over the land portion of the domain and partly over water bodies close to its boundaries.

The climatological seasonal (JJAS) distribution of rainfall over the Indian subcontinent has been discussed in detail in relation to Fig. 4. Differences in seasonal rainfall between PLC and HLC show a significant reduction over a large part of CI, peninsular India, and northwestern India (Fig. 6a). It is interesting to note that the pattern of decrease matches very well with the regions that show an increase in crop PFTs from 1950 to 2005, with maximum changes over the northwest of India. The magnitude of decrease in seasonal rainfall is quite high (by 5–7 cm) over certain regions; however, it is difficult to find out exact reason for such changes at every grid. It may be due to changes in local instability brought about by land–atmosphere feedback processes or changes in large-scale moisture convergence or both. A part of these changes also depend on the choice of parameterization schemes in the RCM. Observational evidence suggests that despite increase in water holding capacity of the atmosphere on a large scale, changes in rainfall are very localized. It is plausible that large-scale conditions and moisture convergence in the PLC experiment might be relatively unfavorable for formation of rainfall compared to the HLC experiment. In order to analyze changes in the large-scale moisture convergence, we calcu-

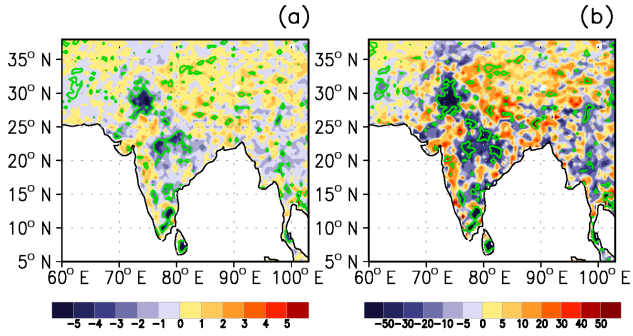

Figure 7. Difference (PLC–HLC) in **(a)** number of moderate rainfall events during JJAS and **(b)** total amount of moderate rainfall (in mm day^{-1}; 1982–2008). Green contour shows differences significant at the 90 % confidence level.

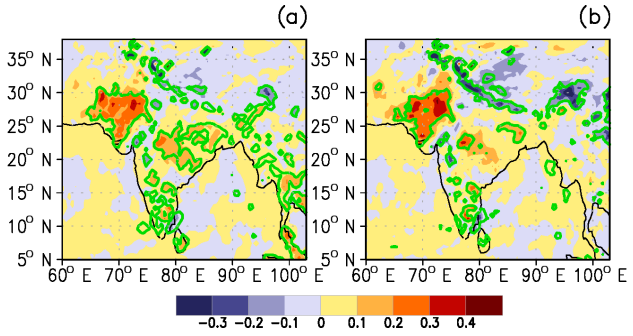

Figure 8. Difference (PLC–HLC) in JJAS-averaged 2 m air temperature (in °C; 1982–2008), for **(a)** daily mean, and **(b)** daily maximum temperature. Green contour shows significance at the 90 % confidence level.

lated vertically integrated moisture flux (qV) from surface to 300 hPa. Following Helmholtz's theorem, velocity potential is further calculated that represents the divergent component of that moisture flux (cf. Behera et al., 1999). From the difference, it turns out that large-scale moisture convergence is reduced in the PLC experiment and contributes to the reduction in rainfall over CI (Fig. 6a). However, it also remains to be explored how much does LULCC contribute to the reduction in surface evaporation and hence moisture convergence over land. This will be discussed in Sect. 4.3 and 4.4. Studies have shown that precipitation variance is amplified by land–atmosphere feedback over those regions that are least affected by SST (cf. Koster et al., 2000). Therefore, it is possible that higher decreases in precipitation over the semi-arid northwestern region of India, that is farther away from the influence of SST, are dominated by changes in local land-surface processes.

As the monsoon circulation in the PLCS experiment is relatively weaker than in the PLC experiment and SSTs are cooler, large-scale moisture flux into the monsoon domain is also expected to be less. Therefore, changes in rainfall over land would better reflect the impact of local land–atmosphere feedbacks due to LULCC. It is evident from Fig. 6b that there is indeed a significant reduction in seasonal rainfall in PLCS, and over a much wider area of CI and the western Ghats region than in PLC. Enhancement of rainfall is also evident over some parts of the north and west of India that depict an increase in forests (Fig. 1e). Decrease in seasonal rainfall, by a maximum of about 3–4 cm is evident over most parts of CI. Decrease in large-scale moisture convergence in the PLCS experiment is also very widespread extending up to the Arabian Sea, and stronger than in PLC experiment (as evident from denser dashed contours).

Changes in frequency of daily rainfall and intensity

We study next how changes in seasonal rainfall over CI are associated with the changes in daily rainfall in the moderate and extreme category. We adopt the criteria for determining thresholds for categorizing moderate and extreme daily rainfall events over CI in the model, that is not exactly the same but is consistent with the method of Goswami et al. (2006). Any daily rainfall total averaged in a grid box is considered as an event. Percentiles of observed (APHRODITE) daily rainfall over CI during JJAS are calculated for the period 1982 until 2007 to identify the value that corresponds to the range of moderate rainfall and lower threshold of extreme rainfall events (see Sect. 3.3). The observed percentiles are then compared with those calculated for the model to categorize daily moderate and extreme rainfall events in the model. In this way, moderate events are identified in the model when $5.34 <$ daily rainfall ≤ 41.72 mm day^{-1} and extreme events are identified when daily rainfall > 59.94 mm day^{-1}. Figure 7a (Fig. 7b) depicts the difference in total number of moderate rainfall events (intensity of rainfall in moderate category) between PLC and HLC experiments during JJAS from 1982 to 2008. Note that for PLC, there is a significant and widespread decrease over CI and the spatial pattern coincides with the increase in crop PFTs in PLC experiment. It can also be noted, that the pattern of decrease matches very well with that of the changes in seasonal rainfall. Following the above methodology, moderate rainfall events are identified in the PLCS and HLCS experiments when $4.97 <$ daily rainfall ≤ 41.62 mm day^{-1}. Likewise, extreme rainfall events are identified when daily rainfall > 59.80 mm day^{-1}. The spatial pattern of changes depict that this decrease takes place over a larger part of CI as well as the BI domain (shown in Fig. 4b). On the contrary, changes in extreme rainfall events or the intensity of rainfall in that category are not found to be significant between PLC and HLC or between PLCS and HLCS, whether analyzed spatially (figure not shown) or in an aggregated sense over CI.

The mean decrease in the number of moderate rainfall events between PLC and HLC is 388, and that between PLCS and HLCS is 450, which are significant at the 90 % level of significance. Over the larger BI domain, decrease in moderate rainfall events between PLC and HLC is even greater and is about 642 (significant at 95 %). We note that the order of decrease is comparable to the observed decrease in the number of moderate rainfall events over CI (about 640) in the last 55 years. Along with the number of events, intensity of rainfall amount in a season in the moderate category also decreases significantly at the 95 % level of significance. The decrease in number of moderate events and corresponding rainfall intensity between PLCS and HLCS is even greater, aided by further reduction in large-scale convergence of moisture apart from local land–atmosphere feedbacks. Therefore, the additional pair of sensitivity experiments with de-trended SSTs further help in establishing our hypothesis. As moderate rainfall events constitute a major portion of the seasonal (JJAS) rainfall ($\sim$ 85 % in observations), we conclude that decrease in seasonal mean rainfall over CI is mainly attributed to differences in the moderate rainfall category due to increase in crop PFTs. Inclusion of light rainfall events ($1 <$ daily rainfall $< 5.34\,\mathrm{mm\,day^{-1}}$) in the analysis along with the moderate category does not change our result. We further investigate changes in surface temperature over land and other associated fluxes in order to better understand the above large-scale changes.

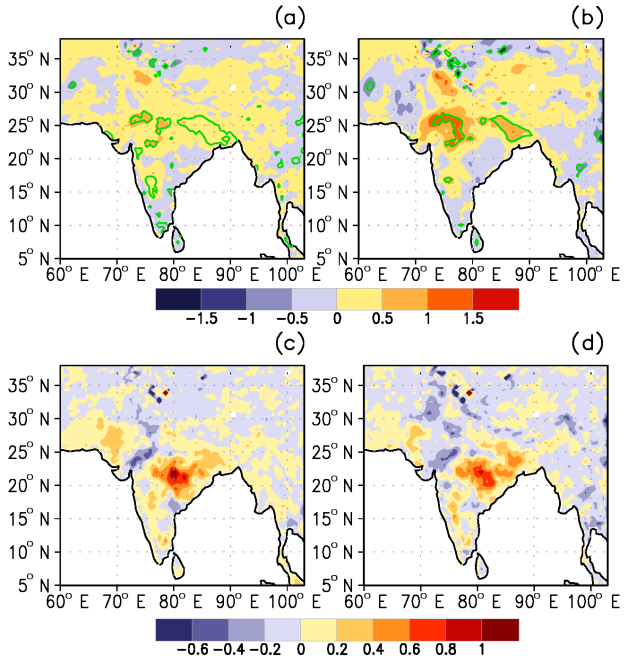

Figure 9. Difference (PLC–HLC) in daily variance of 2 m air temperature in JJAS (in $°C^2$; 1982–2008) for **(a)** daily mean, and **(b)** daily maximum temperature. Green contour shows significance at the 90 % confidence level. Difference (PLC–HLC) in the 90th percentile of daily 2 m air temperature in JJAS (in °C; 1982–2008), for **(c)** daily mean, and **(d)** daily maximum temperature.

4.3 Changes in surface air temperature

4.3.1 PLC and HLC experiments

Daily 2 m mean air temperature during JJAS in PLC is higher than HLC by a maximum of 0.3 °C over CI and parts of south (Fig. 8a). A significant increase in daily maximum temperature (0.4 °C) over the same region as in the mean is also evident (Fig. 8b). The pattern of increase does coincide with increase in crop fraction in PLC (Fig. 1f). Widespread warming is also seen beyond the dry northwestern region of India where the increase in fraction of crop PFTs is more than over CI. Significant cooling is found along a thin belt around the Himalayan foothills in the north that may be attributed to an increase in precipitation (see Fig. 6) as well as changes in albedo and net radiation. A decrease in mean and extreme temperature over small parts of western India is attributed to an increase in forest PFTs (Fig. 1e). At night, the land surface gets de-coupled from the overlying atmosphere on account of cooling, is capped by a layer of inversion and the effect of land-surface processes or vegetation on 2 m temperature is minimized. Therefore, and as discussed in Kothawale et al. (2010), the increase in daily mean temperature is mostly dominated by the increase in daily maximum temperature. However, we also noted an increase in temperature at the 925 hPa level (figure not shown), implying that the surface warming extends further up to the depth of the boundary layer.

Apart from changes in the mean temperature, there are also changes in the variability of daily mean and maximum temperature as evident from Fig. 9a and b. There is significant increase in temperature variability over the central and eastern part of India that is attributed to LULCC as well as changes in surface net radiation and advection of moisture and heat. Increase in the variance of extreme is more widespread than in the mean. As the mean and variance of daily surface temperature are altered over CI, it is expected that daily extremes will also change. In order to find out the differences in the extreme temperatures, percentiles are calculated using a time series of 122 days for 27 years (June–September 1982–2008). Difference in the 90th percentiles of daily mean and maximum temperature (in JJAS) between and PLC and HLC is shown in Fig. 9c and d. The 90th percentiles represent the higher temperature extremes attained within the season in the PLC and HLC experiment. The higher extreme values of both daily mean and maximum temperature are about 1 °C more in the PLC experiment over CI. We note that the area of increase coincides very well with the region of maximum increase in the fraction of crop PFTs from 1950 to 2005 (Fig. 1f). It is also interesting to note that the higher extremes warm by the same order as depicted in observations. Apart from that, the model does not capture the observed warming over

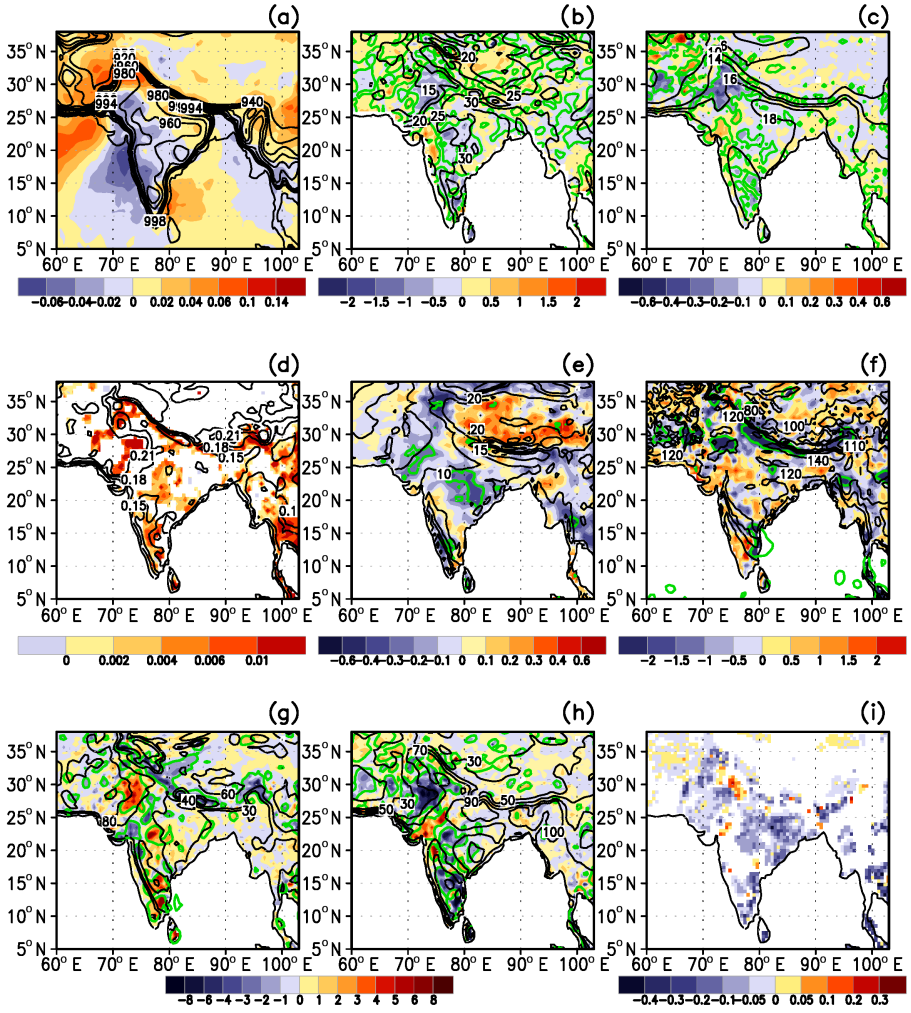

Figure 10. (a) Seasonal (JJAS)-averaged surface pressure in PLC experiment (in black contours) and its difference (PLC–HLC) in shaded color (in hPa; 1982–2008). Green contour shows differences significant at the 90 % confidence level. **(b)–(i)** Show similar differences as in **(a)** but for surface soil moisture (0–10 cm; in mm), 2 m specific humidity (in g kg^{-1}), surface albedo (unitless), total cloud cover (in %), surface net radiation (in W m^{-2}), surface sensible heat flux (in W m^{-2}), surface latent heat flux (in W m^{-2}). **(i)** Shows only the difference (PLC–HLC) in sum of transpiration and evaporation of canopy-intercepted water (in mm day^{-1}). In **(d)** and **(i)**, only the differences significant at the 90 % confidence level are shaded.

the northwestern and peninsular India despite LULCC. Over the northwest of India, the mean as well as extreme temperatures decrease on account of an increase in forest cover over a small region (Fig. 1e).

Changes in other surface variables and cloud cover during JJAS are further analyzed to better understand the causes for surface temperature change. The black contours in different panels in Fig. 10 represent the JJAS mean value from the PLC experiment, while the values in shaded color show the difference. Areas enclosed within the green contours depict changes that are significant. One would expect the surface pressure over land to decrease and an increase in the land–ocean temperature gradient in the PLC experiment on account of an increase in the surface temperature. However, from Fig. 10a it is evident that surface pressure has increased over most of north, northwest, and the Gangetic plains of India in PLC compared to HLC. Although a part of CI and its west shows a decrease in surface pressure, the changes are not significant. Therefore, changes in surface roughness length mainly dominate the increase in surface wind speed, compared to changes in surface pressure. There is also a significant decrease in soil moisture (Fig. 10b) associated with the decrease in precipitation, and specific humidity at 2 m (Fig. 10c) over those regions where the fraction of crop PFTs has increased in PLC.

We note a significant increase in surface albedo over the land part (Fig. 10d) that is attributed to the increase in crop PFTs and reduction in precipitation, that leads to drier soils in the PLC. An increase in albedo would tend to reduce the surface temperature. However, we also find that the cloud cover

has decreased significantly over a large part of CI, the western, northern, and peninsular India in PLC (Fig. 10e). This conforms to the reduction in seasonal precipitation in PLC compared to HLC. Due to reduction in cloud cover, there is also an increase in surface net radiation (NRAD) over those regions, although changes are not found to be significant over CI (Fig. 10f). The increase in NRAD over central and southern India in PLC is contributed by a significant increase in net shortwave (SW) radiation. Whereas, the decrease in NRAD over the Himalayan foothills is associated with a significant decrease in both net SW and longwave (LW) radiation. Over CI, decrease in net LW radiation partly compensates for the increase in net SW radiation in PLC (figure not shown); hence, changes in NRAD are small. Decrease in net LW radiation in PLC dominates over the northwest of India. The increased NRAD in PLC further contributes to a significant enhancement (reduction) in the mean surface sensible heat flux (SHF) over those areas that show an increase in crop (forest) cover (Fig. 10g). On the contrary, latent heat flux (LHF) that is directly associated with the ET shows significant changes in the opposite sense (Fig. 10h), leading to an overall enhancement in the Bowen ratio in PLC (figure not shown). Therefore, we infer that an increase in NRAD and SHF in PLC dominates over changes in surface albedo over India south of 30° N and contributes to the increase in surface temperature. Our results also conform to the inferences reported in earlier studies (Lawrence and Chase, 2010; Sampaio et al., 2007; Davin and De Noblet-Ducoudrè, 2010).

It is interesting to note that about 30 % of the changes in LHF over CI, western, and southern India in PLC (Fig. 10h) are mainly contributed by a reduction in transpiration from vegetation and evaporation of canopy-intercepted water due to LULCC (Fig. 10i). Although this decrease is relatively higher over eastern India than towards CI, enhanced ground evaporation arising from increased precipitation in PLC (compared to HLC) partly compensates for that decrease. As a result changes in total ET are not significant towards the east of India. Therefore, due to a reduction in surface ET, the increased NRAD absorbed at the surface over central and southern India is primarily used in enhancing the SHF and that further contributes to the increase in mean and higher extreme surface temperatures in PLC during JJAS. As mentioned in the introduction, the daily spatiotemporal variability of surface temperature may be attributed to local thermodynamic effects due to changes in low-level moisture and surface fluxes as well as large-scale dynamics. In this regard, we note that our results differ from earlier studies that have shown a decrease in growing season surface temperatures over India due to irrigated crops (e.g., Sen Roy et al., 2007; Lee et al., 2009) because we did not use any parameterization scheme for irrigation. Irrigation provides an enhanced source of soil moisture and hence cools the surface and lowers the temperature due to evaporation.

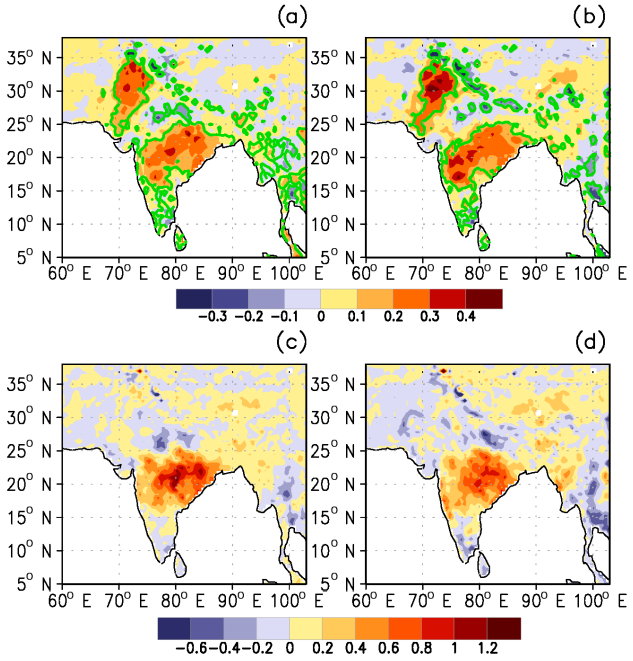

Figure 11. Difference (PLCS–HLCS) in seasonal (JJAS)-averaged 2 m air temperatures (in °C; 1982–2008) for **(a)** daily mean, and **(b)** daily maximum temperature. Green contour shows differences significant at the 90 % confidence level. Difference (PLCS–HLCS) in the 90th percentile of daily 2 m air temperature in JJAS (in °C; 1982–2008), for **(c)** daily mean, and **(d)** daily maximum temperature.

4.3.2 PLCS and HLCS experiment

We find similar changes when simulated surface temperatures in the PLCS and HLCS experiments are compared. Daily 2 m mean as well as maximum temperature are significantly enhanced in the PLCS experiment by maximum of 0.5 °C, but over a much larger area covering central and southern parts of India compared to HLCS (Fig. 11a and b). We note that the increase in temperature over CI due to similar LULCC is higher and more widespread than in PLC. Likewise, over the northwest of India, the spatial pattern of increase extends further to the north and shows higher increase (0.5 °C) in the maximum. Significant cooling is also evident over western and northern India in PLCS over those areas that show increase in forest cover. The higher extremes, i.e., 90th percentiles of the daily mean (maximum) temperature, have also increased in the PLCS experiment by 1.2 °C (1.0 °C), which is more than in the earlier set of experiments PLC and HLC (Fig. 11c and d). Increase in higher extreme temperature in the PLCS experiment extends further to the west and hence covers a much larger part of CI than in the PLC experiment. We further note that the order of increase in temperature as evident from these two experiments is comparable to that inferred from observations.

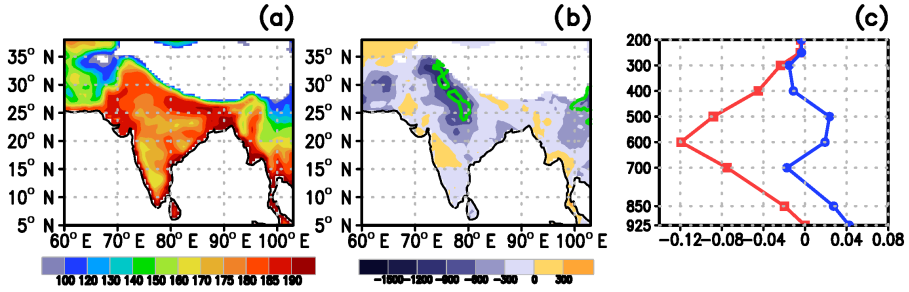

Figure 12. (a) Seasonal average (JJAS) of vertically integrated moist static energy (VIMSE; surface – 500 hPa) in PLC experiment (in 1×10^4 kJ kg^{-1}; 1982–2008). **(b)** Difference (PLC–HLC) in VIMSE (in kJ kg^{-1}; 1982–2008). Green contour shows differences significant at the 90 % confidence level. **(c)** Difference (PLC–HLC) in CI-averaged moist static energy (MSE; in red) and dry static energy (DSE; in blue) in units of 1×10^3 kJ kg^{-1}.

There are significant and widespread decreases in soil moisture, LHF, and specific humidity but increases in NRAD and sensible heat flux in the PLCS experiment compared well to HLCS (figures not shown) that contribute to the increase in surface temperature. It is interesting that in both sets of experiments, the increase in surface temperature is slightly towards the south of the area that depicts an increase in observations. Apart from that, mean monsoonal features simulated in the PLCS experiment also convey that there is a decrease in large-scale moisture flow as well as precipitation over the land. As a result alterations in net radiation and surface fluxes between PLCS and HLCS experiments have a greater impact on changes in surface air temperature. Therefore, our experiments with de-trended SST further confirm the proposition that LULCC has partly contributed to the observed increase in surface temperature from 1951 to 2005.

4.4 Physical mechanisms

After analyzing the changes in surface variables and the large-scale in the set of model experiments, one pertinent question arises. How does LULCC lead to a reduction in moderate rainfall events? Halder et al. (2015) showed that surface ET can strongly modulate the terrestrial segment of land–atmosphere coupling strength (Dirmeyer, 2011) and the chances of triggering of convection and precipitation during the Indian summer monsoon. From comparison of the PLC and HLC experiments, we note a decrease of about 3 cm in the total evapotranspiration over CI, that is 40–60 % of the maximum decrease in the total rainfall magnitude. Although an increase in crop cover and decrease in forest increases the temperature near the surface and within the boundary layer, the associated decrease in local moisture flux could possibly also lower the large-scale convective instability. To better understand that, we analyze changes in vertically integrated moist static energy (VIMSE), which is a good measure of instability and precipitation in the tropics (Srinivasan and Smith, 1996). VIMSE from surface to 500 hPa during JJAS in PLC depicts high values over those areas of land that show maximum seasonal mean rainfall (Fig. 12a). Differences show that there is a large-scale reduction in VIMSE in the PLC experiment, with significant decreases over a major part of CI and the north (Fig. 12b). Additionally, the difference (PLC–HLC) in the vertical profile of dry static energy (DSE, blue line) suggests an increase in temperature in the lower levels of the troposphere over CI. Despite that, the effect of decreased moisture in the lower levels effectively reduces the MSE (red line, Fig. 12c) thereby increasing atmospheric stability and hence lowering the chances of triggering of moist convection over land in the PLC experiment. Reduced large-scale low-level moisture convergence over the land part in the PLC than HLC, on account of a reduction in surface roughness length (Fig. 6a) also contributes to the reduction in convective instability. These two factors together reduce rainfall in the moderate category.

5 Discussions

This study explores the hypothesis how LULCC over India has contributed to the observed decrease in moderate rainfall events over CI and increase in extreme daily surface temperatures during the monsoon season, from 1951 to 2005, using a RCM. The climatological mean features of Indian summer monsoon are very well captured by the RCM RegCM4. The statistics of differences between the long simulations with fixed present-day (2005) and historical (1950) PFT distributions, LAIs, and SAIs demonstrate the impact of LULCC on daily surface temperature and precipitation variability during the monsoon season (JJAS). Another two similar experiments are also conducted, but with SSTs de-trended within the RCM domain in order to eliminate the effect of the positive trend in Indian Ocean SSTs on temperature and precipitation changes over land.

Differences show that seasonal rainfall and large-scale moisture convergence are significantly decreased in the PLC and PLCS experiments when compared to the HLC and HLCS experiments, respectively. The decrease is enhanced in the case of the PLCS experiment compared to PLC. That

decrease in seasonal rainfall is mostly contributed by a significant decrease in moderate rainfall events and amount over CI. Changes in extreme rainfall events are not significant. We demonstrate that a significant increase in surface wind speed over land is responsible for the decrease in moisture convergence. The increase in surface wind speed is attributed to an increase in crop cover at the expense of forests and hence a reduction in surface roughness length. This way, the dynamical response of regional climate over India to LULCC is demonstrated. Decreases in forest cover and increases in crops between 1950 and 2005 also lead to reductions in the regional moisture flux emanating from the surface significantly. Therefore, despite significant increases in surface and boundary layer temperature, a decrease of moisture reduces the large-scale convective instability and chances of triggering of convection and hence precipitation over central and northern India. This mechanism constitutes the thermodynamic response of the regional climate to LULCC. A decrease in total cloud cover increases the surface net radiation, which together with a decrease in surface moisture results in an increase in the surface sensible heat flux and the Bowen ratio. Together, these changes contribute to the increase in mean surface temperature and its extremes. It is noteworthy that the order of increase in surface temperature extremes over India during the summer monsoon season is comparable to that of the observed changes when de-trended SSTs within the model domain are used. Likewise, the order of decrease in moderate rainfall events over CI also become comparable to the observed changes during the period 1951–2005.

It is important to note that the deficiency in the RCM in terms of capturing the frequency distribution of daily very heavy rainfall events over CI realistically could have a bearing on our inferences. Hence, our results are partly dependent on the choice of model parameterization schemes. However, this is a well-known problem related to climate models (Frei et al., 2003; Kang et al., 2014) and similar studies when repeated with other RCMs is expected to give us further evidence on the role of LULCC in affecting the frequency distribution of daily rainfall events over India. Apart from that, the criteria used for calculating thresholds for daily moderate and extreme rainfall events in the RCM may also have influence on the results. There is a cold temperature bias over land in the model RegCM4, and positive rainfall bias over the ocean (figure not shown), which is also evident from earlier studies (Saha et al., 2011, 2012; Halder et al., 2015). Apparently, in all these experiments the global warming signal is also present in the large-scale LBCs used from NCEP/NCAR reanalysis that force the model in one way only. A part of the change in simulated surface temperature and rainfall in the model may also be attributed to non-linear interactions (internal variability) that is model dependent. However, we expect the differences between two simulations with the same model to reduce the effect of these factors and demonstrate the impact of LULCC on regional climate over India. Use of a high-resolution RCM is more advantageous in excluding large-scale remote feedbacks that take place in a coarse-resolution GCM and therefore helps to better resolve regional land–atmosphere feedbacks. Apart from that, we believe that the land cover data prepared from multiple sources and used as fixed lower boundary condition in this study is much improved compared to other historical reconstructed data utilized in earlier studies. Nonetheless, our experiments demonstrate that the decrease in moderate rainfall events over central India is partly attributed to changes in land-use/land-cover from 1950 to 2005.

6 Conclusions

Apart from an accelerated warming trend in the global mean surface temperature in the later half of the 20th century, the number of extreme events in terms of temperature as well as precipitation has been reported to increase. As regional or local changes in these extremes in different seasons can have different signatures due to complex regional feedbacks associated with the GHGs, clouds, aerosols, and other anthropogenic activities such as LULCC, they need greater attention and proper attribution. Regional land–atmosphere feedbacks associated with LULCC are one of the potential drivers of climate change. Land cover data show significant decrease in the forest and increase in crop cover over central, south, and northwest part of India between 1950 and 2005. From 1951 to 2005, the observed mean (extreme) surface temperature over India has increased by a maximum of 1.11 °C (1.48 °C) during the summer monsoon season. There have also been significant changes in the rainfall distribution during those 55 years. While observed heavy and very heavy precipitation events have increased over central India, due to a significant decrease in moderate rainfall events, the overall seasonal rainfall has reportedly remained stable during that period. In this study, we cannot reject the hypothesis that LULCC over India has partly contributed to the observed decrease in moderate rainfall events and increase in extreme surface temperature during the summer monsoon season.

It is found that increase in mean and extreme surface temperatures by 1–1.2 °C over CI in the present land cover experiment coincides with the region of decrease in forest and increase in crop type of PFTs. Furthermore, increase is found to be even higher and more widespread over the Indian region when the positive trend in the Indian Ocean SSTs is removed. There is a reduction in large-scale convective instability and moisture convergence over land that leads to decrease in seasonal precipitation in the PLC experiment compared to HLC. As the major portion of monsoon seasonal rainfall occurs through moderate rainfall events (Goswami et al., 2006), it is expected that the decrease in moisture flux and large-scale convective instability over land would also lead to a decrease in the moderate rainfall category. The model results indeed support our hypothesis, and show that regions with a decrease in forest cover also depict a decrease in the number

of moderate rainfall events as well as the amount of rainfall in that category. Changes in heavy rainfall events are not found to be significant. These results are further supported by the two additional sensitivity experiments: PLCS and HLCS. We conclude that changes in local/regional moisture flux and surface roughness length that are associated with this type of LULCC are crucial in determining the changes in large-scale instability and moisture convergence over land and the frequency distribution of daily rainfall events over the Indian monsoon region. Therefore, this study demonstrates that LULCC in the last 55 years have contributed partly to the observed decrease in moderate rainfall events over India as well as increase in extreme surface temperatures.

Understanding the mechanisms responsible for observed changes in daily rainfall distribution and extreme surface temperature in the monsoon regions is important for the scientific community and policy makers as well. It is conceivable that, as the global mean temperature becomes warmer and the regional climates possibly more unpredictable, LULCC due to population growth, deforestation/afforestation, agricultural expansion, and urbanization would add more uncertainties through its dynamic (changes in large-scale circulation) and thermodynamic effects (albedo, evaporation, and instability changes). However, this study does not include urbanization effects. Apart from that, impact of aerosols, GHGs and irrigation activity have also not been considered here which would introduce competing influences. Therefore, part of the regional warming over India seen in observations could not be explained only through LULCC that we have isolated here. Investigation of the impact of LULCC in a high-resolution coupled global climate model where the land cover changes with time or dynamic vegetation is used, would make another interesting study. Furthermore, studies similar as this with a suite of climate models would further augment our understanding about the role of LULCC in Indian monsoon climate. Nevertheless, this study shows that it is highly important to include projected anthropogenic changes in regional land-use/land-cover in IPCC future climate change scenarios.

The Supplement related to this article is available online at doi:10.5194/hess-20-1765-2016-supplement.

Acknowledgements. Authors thank the Abdus Salam International Centre for Theoretical Physics in Trieste, Italy, for making the model codes of RegCM4.0 available for this study from http://gforge.ictp.it/gf/. Global time varying forcing data sets for the RCM and fixed data sets for the CLM3.5 land-surface model are obtained from http://users.ictp.it/ pubregcm/RegCM4/globedat.htm. The PFT-based global vegetation data sets were prepared at the Cooperative Institute for Research in Environmental Sciences, University of Colorado at Boulder, USA. Daily high-resolution gridded temperature data (product no. 3/2008) prepared from quality controlled station observations can be purchased for a fee from the National Climate Centre (NCC), IMD, Pune, India. Details about the procedure of purchase can be searched in the link "NCC Gridded Data Product", present in the webpage http://www.imdpune.gov.in/library/Data_Sale.html. The figures have been prepared using the freely available software package GrADS http://cola.gmu.edu/grads/downloads.php.

Authors gratefully acknowledge the use of data and resources at the Indian Institute of Tropical Meteorology, Pune, India. Fellowship of S. Halder was funded by the CSIR, New Delhi, India, during completion of this study for his PhD thesis while at IITM. S. Halder and P. Dirmeyer are supported by a grant from the Ministry of Earth Sciences, Govt. of India to the Center for Ocean–Land–Atmosphere Studies of George Mason University. Support for the Twentieth Century Reanalysis Project data set is provided by the US Department of Energy, Office of Science Innovative and Novel Computational Impact on Theory and Experiment (DOE INCITE) program, and Office of Biological and Environmental Research (BER), and by the National Oceanic and Atmospheric Administration Climate Program Office.

Edited by: W. Buytaert

References

Adler, R. F., Huffman, G. J., Chang, A., Ferraro, R., Xie, P., Janowiak, J., Rudolf, B., Schneider, U., Curtis, S., Bolvin, D., Gruber, A., Susskind, J., and Arkin, P.: The version 2 Global Precipitation Climatology Project (GPCP) monthly precipitation analysis (1979–present), J. Hydrometeorol., 4, 1147–1167, doi:10.1175/1525-7541(2003)004<1147:TVGPCP>2.0.CO;2, 2003.

Alexander, L. V., Zhang, X., Peterson, T. C., Caesar, J., Gleason, B., Tank, A. M. G. K., Haylock, M., Collins, D., Trewin, B., Rahimzadeh, F., Tagipour, A., Kumar, K. R., Revadekar, J., Griffiths, G., Vincent, L., Stephenson, D. B., Burn, J., Aguilar, E., Brunet, M., Taylor, M., New, M., Zhai, P., Rusticucci, M., and Vazquez-Aguirre, J. L.: Global observed changes in daily climate extremes of temperature and precipitation, J. Geophys. Res., 111, D05109, doi:10.1029/2005JD006290, 2006.

Ali, H., Misra, V., and Pai, D. S.: Observed and projected urban extreme rainfall events in India, J. Geophys. Res., 19, 12621–12642, doi:10.1002/2014JD022264, 2014.

Allen, M. R. and Ingram, W. J.: Constraints on future changes in climate and the hydrologic cycle, Nature, 419, 224–231, doi:10.1038/nature01092, 2002.

Avila, F. B., Pitman, A. J., Donat, M. G., Alexander, L. V., and Abramowitz, G.: Climate model simulated changes in temperature extremes due to land cover change, J. Geophys. Res., 117, D04108, doi:10.1029/2011JD016382, 2012.

Behera, S. K., Krishnan, R., and Yamagata, T.: Unusual ocean atmosphere conditions in the tropical Indian ocean during 1994, Geophys. Res. Lett., 26, 3001–3004, doi:10.1029/1999GL010434, 1999.

Bonan, G. B., Oleson, K. W., Vertenstein, M., Levis, S., Zeng, X., Dai, Y., Dickinson, R. E., and Yang, Z.-L.: The land surface climatology of the community land model coupled to the NCAR community climate model, J. Climate, 15, 3123–3149,

doi:10.1175/1520-0442(2002)015<3123:TLSCOT>2.0.CO;2, 2002.

Bounoua, L., DeFries, R., Collatz, G. J., Sellers, P., and Khan, H.: Effects of land cover conversion on surface climate, Climatic Change, 52, 29–64, 2002.

Chow, K. C., Cha, J. C. L., Pal, J. S., and Giorgi, F.: Convection suppression criteria applied to the MIT cumulus parameterization scheme for simulating the Asian summer monsoon, Geophys. Res. Lett., 32, L24709, doi:10.1029/2006GL028026, 2006.

Chowdary, J. S., John, N., and Gnanaseelan, C.: Interannual variability of surface air-temperature over India: impact of ENSO and Indian Ocean Sea surface temperature, Int. J. Climatol., 34, 416–429, doi:10.1002/joc.3695, 2013.

Compo, G. P., Whitaker, J. S., Sardeshmukh, P. D., Matsui, N., Allan, R. J., Yin, X., Gleason, B. E., Vose, R. S., Rutledge, G., Bessemoulin, P., Bronnimann, S., Brunet, M., Crouthamel, R. I., Grant, A. N., Groisman, P. Y., Jones, P. D., Kruk, M. C., Kruger, A. C., Marshall, G. J., Maugeri, M., Mok, H. Y., Nordli, Ø., Ross, T. F., Trigo, R. M., Wang, X. L., Woodruff, S. D., and Worleyu, S. J.: Review article: the Twentieth Century Reanalysis Project, Q. J. Roy. Meteorol. Soc., 137, 1–28, doi:10.1002/qj.776, 2011.

Davin, E. L. and De Noblet-Ducoudrè, N.: Climatic impact of global-scale deforestation: radiative versus nonradiative processes, J. Climate, 23, 97–112, 2010.

Dirmeyer, P. A.: The terrestrial segment of soil moisture-climate coupling, Geophys. Res. Lett., 38, L16702, doi:10.1029/2011GL048268, 2011.

Dirmeyer, P. A., Niyogi, D., de Noblet-Ducoudrè, N., Dickinson, R. E., and Snyder, P. K.: Editorial: impacts of land use change on climate, Int. J. Climatol., 30, 1905–1907, 2010.

Douglas, E. M., Niyogi, D., Frolking, S., Yeluripati, J. B., Pielke Sr., R. A., Vorosmarty, C. J., and Mohanty, U. C.: Change in moisture and energy fluxes due to agricultural land use and irrigation in the Indian monsoon belt, Geophys. Res. Lett., 33, L14403, doi:10.1029/2006GL026550, 2006.

Douglas, E. M., Beltran-Przekurat, A., Niyogi, D., Pielke Sr., R. A., and Vörösmarty, C., J.: The impact of agricultural intensification and irrigation on land-atmosphere interactions and Indian monsoon precipitation – A mesoscale modeling perspective, Global Planet. Change, 67, 117–128, doi:10.1016/j.gloplacha.2008.12.007, 2009.

Dutta, S. K., Das, S., Kar, S. C., Mohanty, U. C., and Joshi, P. C.: Impact of vegetation on the simulation of seasonal monsoon rainfall over the Indian subcontinent using a regional model, J. Earth Syst. Sci., 118, 413–440, 2009.

Elguindi, N., Bi, X., Giorgi, F., Nagarajan, B., Pal, J., Solmon, F., Rauscher, S., and Zakey, A.: RegCM version 4.0 User's Guide, ICTP, Trieste, Italy, available at: gforge.ictp.it/gf/download/docmanfileversion/6/253/UserGuide.pdf (last access: June 2015), 2010.

Feddema, J., Oleson, K., Bonan, G., Mearns, L., Washington, W., Meehl, G., and Nychka, D.: A comparison of a GCM response to historical anthropogenic land cover change and model sensitivity to uncertainty in present-day land cover representations, Clim. Dynam., 25, 581–609, doi:10.1007/s00382-005-0038-z, 2005.

Feser, F. and Barcikowska, M.: The influence of spectral nudging on typhoon formation in regional climate models, Environ. Res. Lett., 7, 014024, doi:10.1088/1748-9326/7/1/014024, 2012.

Feser, F., Rockel, B., von Storch, H., Winterfeldt, J., and Zahn, M.: Regional climate models add value to global model data: a review and selected examples, B. Am. Meteorol. Soc., 92, 1181–1192, doi:10.1175/2011BAMS3061.1, 2011.

Frei, C., Christensen, J. H., Déqué, M., Jacob, D., Jones, R. G., and Vidale, P. L.: Daily precipitation statistics in regional climate models: evaluation and intercomparison for the European Alps, J. Geophys. Res., 108, 4124, doi:10.1029/2002JD002287, 2003.

Fritsch, J. M. and Chappell, C. F.: Numerical prediction of convectively driven mesoscale pressure systems. Part I: Convective parameterization, J. Atmos. Sci., 37, 1722–1733, doi:10.1175/1520-0469(1980)037<1722:NPOCDM>2.0.CO;2, 1980.

Garratt, J. R.: Sensitivity of climate simulations to land-surface and atmospheric boundary layer treatments – a review, J. Climate, 6, 419–449, doi:10.1175/1520-0442(1993)006<0419:SOCSTL>2.0.CO;2, 1993.

Giorgi, F. and Bates, G. T.: The climatological skill of a regional model over complex terrain, Mon. Weather Rev., 117, 2325–2347, 1989.

Giorgi, F. and Mearns, L. O.: Introduction to special section: Regional climate modeling revisited, J. Geophys. Res., 104, 6335–6352, 1999.

Giorgi, F., Coppola, E., Solmon, F., Mariotti, L., Sylla, M. B., Bi, X., Elguindi, N., Diro, G. T., Nair, V., Giuliani, G., Turuncoglu, U. U., Cozzini, S., Guttler, I., O'Brien, T. A., Tawfik, A. B., Shalaby, A., Zakey, A. S., Steiner, A. L., Stordal, F., Sloan, L. C., and Brankovic, C.: RegCM4: model description and preliminary tests over multiple CORDEX domains, Clim. Res., 52, 7–29, doi:10.3354/cr01018, 2012.

Goldewijk, K. K.: Estimating global land use change over the past 300 years: the HYDE database, Global Biogeochem. Cy., 15, 417–433, 2001.

Goswami, B. N., Venugopal, V., Sengupta, D., Madhusoodanan, M. S., and Xavier, P. K.: Increasing trend of extreme rain events over India in a warming environment, Science, 314, 1442–1445, doi:10.1126/science.1132027, 2006.

Grell, G. A.: Prognostic evaluation of assumptions used by cumulus parameterization, Mon. Weather. Rev., 121, 764–787, doi:10.1175/1520-0493(1993)121<0764:PEOAUB>2.0.CO;2, 1993.

Haerter, J. O. and Berg, P.: Unexpected rise in extreme precipitation caused by a shift in rain type?, Nat. Geosci., 2, 372–373, doi:10.1038/ngeo523, 2009.

Halder, S., Dirmeyer, P., and Saha, S. K.: Uncertainty in the mean and variability of Indian summer monsoon due to land atmosphere feedback in RegCM4, J. Geophys. Res., 120, 9437–9458, doi:10.1002/2015JD023101, 2015.

Holtslag, A. A. M., Bruijn, E. I. F. D., and Pan, H. L.: A high resolution air mass transformation model for short-range weather forecasting, Mon. Weather. Rev., 118, 1561–1575, doi:10.1175/1520-0493(1990)118<1561:AHRAMT>2.0.CO;2, 1999.

Hurtt, G. C., Frolking, S., Fearon, M., Moore, B., Shevliakova, E., Malyshev, S., Pacala, S., and Houghton, R.: The underpinnings of land-use history: three centuries of global gridded land-use transitions, wood-harvest activity, and resulting secondary lands, Global Change Biol., 12, 1208–1229, doi:10.1111/j.1365-2486.2006.01150.x, 2006.

Jaswal, A. K., Rao, G. P., and De, U.: Spatial and temporal characteristics of evaporation trends over India during 1971–2000, Mausam, 59, 149–158, 2008.

Jaswal, A. K., Rao, P. C. S., and Singh, V.: Climatology and trends of summer high temperature days in India during 1969–2013, J. Earth Syst. Sci., 124, 1–15, 2015.

Kalnay, E., Kanamitsu, M., Kistler, R., Collins, W., Deaven, D., Gandin, L., Iredell, M., Saha, S., White, G., Woollen, J., Zhu, Y., Leetmaa, A., Reynolds, R., Chelliah, M., Ebisuzaki, W., Higgins, W., Janowiak, J., Mo, K. C., Ropelewski, C., Wang, J., Jenne, R., and Joseph, D.: The NCEP/NCAR 40-year reanalysis project, B. Am. Meteorol. Soc., 77, 437–470, 1996.

Kang, I.-S., Yang, Y. M., and Tao, W. K.: GCMs with implicit and explicit representation of cloud microphysics for simulation of extreme precipitation frequency, Clim. Dynam., 45, 325–335, doi:10.1007/s00382-014-2376-1, 2014.

Kiehl, J. T., Hack, J. J., Bonan, G. B., Boville, B. A., Briegleb, B. P., Williamson, D. L., and Rasch, P. J.: Description of the NCAR Community Climate Model (CCM3), Tech. Rep. NCAR/TN-420+STR, NCAR, Boulder, Colorado, USA, 152 pp., 1996.

Kishtawal, C., Niyogi, D., Tewari, M., Pielke Sr., R. A., and Shepherd, M.: Urbanization signature in the observed heavy rainfall climatology over India, Int. J. Climatol., 30, 1908–1916, doi:10.1002/joc.2044, 2009.

Koster, R. D., Suarez, M. J., and Heiser, M.: Variance and predictability of precipitation at seasonal-to-interannual timescales, J. Hydrometeorol., 1, 26–46, doi:10.1175/1525-7541(2000)001<0026:VAPOPA>2.0.CO;2, 2000.

Kothawale, D. R. and Rupa Kumar, K.: On the recent changes in surface temperature trends over India, Geophys. Res. Lett., 32, L18714, doi:10.1029/2005GL023528, 2005.

Kothawale, D. R., Munot, A. A., and Kumar, K. K.: Surface air temperature variability over India during 1901–2007, and its association with ENSO, Clim. Res., 42, 89–104, doi:10.3354/cr00857, 2010.

Krishnan, R. and Ramanathan, V.: Evidence of surface cooling from absorbing aerosols, Geophys. Res. Lett., 29, 89–104, doi:10.1029/2002GL014687, 2002.

Krishnan, R., Sabin, T. P., Vellore, R., Mujumdar, M., Sanjay, J., Goswami, B. N., Hourdin, F., Dufresne, J. -L., and Terray, P.: Deciphering the desiccation trend of the South Asian monsoon hydroclimate in a warming world, Clim. Dynam., 1–21, doi:10.1007/s00382-015-2886-5, 2015.

Laprise, R., de Elía, R., Caya, D., Biner, S., Lucas-Picher, P., Diaconescu, E., Leduc, M., Alexandru, A., and Separovic, L.: Challenging some tenets of regional climate modeling, Meteorol. Atmos. Phys., 100, 3–22, 2008.

Lawrence, P. J. and Chase, T. N.: Investigating the climate impacts of global land cover change in the community climate system model, Int. J. Climatol., 30, 2066–2087, doi:10.1002/joc.2061, 2010.

Leduc, M. and Laprise, R.: Regional climate model sensitivity to domain size, Clim. Dynam., 32, 833–854, 2009.

Lee, E., Chase, T. N., Rajagopalan, B., Barry, R. G., Biggs, T. W., and Lawrence, P. J.: Effects of irrigation and vegetation activity on early Indian summer monsoon variability, Int. J. Climatol., 29, 573–581, doi:10.1002/joc.1721, 2009.

Lei, M., Niyogi, D., Kishtawal, C., Pielke Sr., R. A., Beltrán-Przekurat, A., Nobis, T. E., and Vaidya, S. S.: Effect of explicit urban land surface representation on the simulation of the 26 July 2005 heavy rain event over Mumbai, India, Atmos. Chem. Phys., 8, 5975–5995, doi:10.5194/acp-8-5975-2008, 2008.

Lohar, D. and Pal, B.: The effect of irrigation on premonsoon season over South West Bengal, India, J. Climate, 8, 2567–2570, doi:10.1175/1520-0442(1995)008<2567:TEOIOP>2.0.CO;2, 1995.

Mahmood, R., Pielke Sr., R. A., Hubbard, K., Niyogi, D., Dirmeyer, P., McAlpine, C., Carleton, A., Hale, R., Gameda, S., Beltran-Przekurat, A., Baker, B., McNider, R., Legates, D. R., Shepherd, M., Du, J., Blanken, P., Frauenfeld, O. W., Nair, U. S., and Fall, S.: Land cover changes and their biogeophysical effects on climate, Int. J. Climatol., 34, 929–953, 2014.

Nayak, S. and Mandal, M.: Impact of land-use and land-cover changes on temperature trends over Western India, Curr. Sci. India, 102, 1166–1173, 2012.

Niranjan, Kumar, K., Rajeevan, M., Pai, D. S., Srivastava, A. K., and Preethi, B.: On the observed variability of monsoon droughts over India, Weather Clim. Extr., 1, 42–50, doi:10.1016/j.wace.2013.07.006, 2013.

Niyogi, D., Chang, H. -I., Chen, F., Gu, L., Kumar, A., Menon, S., and Pielke Sr., R., A.: Potential impacts of aerosol-land-atmosphere interactions on the Indian monsoonal rainfall characteristics, Natural Hazards, Special Issue on Monsoons, Invited Contrib., 42, 345–359, doi:10.1007/s11069-006-9085-y, 2007.

Niyogi, D., Kishtawal, C. M., Tripathi, S., and Govindaraju, R. S.: Observational evidence that agricultural intensification and land use change may be reducing the Indian summer monsoon rainfall, Water Resour. Res., 46, W03533, doi:10.1029/2008WR007082, 2010.

Oleson, K. W., Niu, G. Y., Yang, Z. L., Lawrence, D. M., Thornton, P. E., Lawrence, P. J., Stockli, R., Dickinson, R. E., Bonan, G. B., Levis, S., Dai, A., and Qian, T.: Improvements to the Community Land Model and their impact on the hydrological cycle, J. Geophys. Res., 113, G01021, doi:10.1029/2007JG000563, 2008.

Oleson, K. W., Lawrence, D. M., Bonan, G. B., Flanner, M. G., Kluzek, E., Lawrence, P. J., Levis, S., Swenson, S. C., Thornton, P. E., Dai, A., Decker, M., Dickinson, R., Feddema, J., Heald, C. L., Hoffman, F., Lamarque, J. F., Mahowald, N., Niu, G. Y., Qian, T., Randerson, J., Running, S., Sakaguchi, K., Slater, A., Stockli, R., Wang, A., Yang, Z. L., Zeng, X., and Zeng, X.: Technical description of version 4.0 of the Community Land Model (CLM), NCAR Technical Note NCAR/TN-387+STR, NCAR, Boulder, Colorado, USA, 257 pp., 2010.

Pai, D. S. and Sridhar, L.: Long term trends in the extreme rainfall events over India, in: High-Impact Weather Events over the SAARC Region, edited by: Ray, K., Mohapatra, M., Bandyopadhyay, B. K., and Rathore, L. S., Springer International Publishing, Cham, Switzerland with Capital Publishing Company, New Delhi, India, 229–240, 2015.

Pai, D. S., Nair, S. A., and Ramanathan, A. N.: Long term climatology and trends of heat waves over India during the recent 50 years (1961–2010), Mausam, 64, 585–604, 2013.

Panda, D. K. and Kumar, A.: The changing characteristics of monsoon rainfall in India during 1971–2005 and links with large scale circulation, Int. J. Climatol., 3881–3899, doi:10.1002/joc.3948, 2014.

Pielke Sr., R. A.: Influence of the spatial distribution of vegetation and soils on the prediction of cumulus convective rainfall, Rev. Geophys., 39, 151–177, doi:10.1029/1999RG000072, 2001.

Pielke Sr., R. A., Pitman, A., Niyogi, D., Mahmood, R., McAlpine, C., Hossain, F., Goldewijk, K. K., Nair, U., Betts, R., Fall, S., Reichstein, M., Kabat, P., and de Noblet, N.: Land use/land cover changes and climate: modeling analysis and observational evidence, WIREs Climate Change, 2, 828–850, doi:10.1002/wcc.144, 2011.

Pitman, A. J., de Noblet-Ducoudré, N., Avila, F. B., Alexander, L. V., Boisier, J.-P., Brovkin, V., Delire, C., Cruz, F., Donat, M. G., Gayler, V., van den Hurk, B., Reick, C., and Voldoire, A.: Effects of land cover change on temperature and rainfall extremes in multi-model ensemble simulations, Earth Syst. Dynam., 3, 213–231, doi:10.5194/esd-3-213-2012, 2012.

Rajeevan, M., Bhate, J., Kale, J. D., and Lal, B.: High resolution daily gridded rainfall data for Indian region: analysis of break and active monsoon spells, Curr. Sci. India, 9, 296–306, 2006.

Rajeevan, M., Bhate, J., and Jaswal, A. K.: Analysis of variability and trends of extreme rainfall events over India using 104 years of gridded daily rainfall data, Geophys. Res. Lett., 35, L18707, doi:10.1029/2008GL035143, 2008.

Ramankutty, N. and Foley, J. A.: Estimating historical changes in global land cover: croplands from 1700 to 1992, Global Biogeochem. Cy., 13, 997–1027, doi:10.1029/1999GB900046, 1999.

Ramankutty, N., Evan, A. T., Monfreda, C., and Foley, J. A.: Farming the planet: 1. Geographic distribution of global agricultural lands in the year 2000, Global Biogeochem. Cy., 22, GB1003, doi:10.1029/2007GB002952, 2008.

Ratnam, J. V., Giorgi, F., Kaginalkar, A., and Cozzini, S.: Simulation of the Indian monsoon using the RegCM3-ROMS regional coupled model, Clim. Dynam., 33, 119–139, doi:10.1007/s00382-008-0433-3, 2009.

Reynolds, R. W., Rayner, N. A., Smith, T. M., Stokes, D. C., and Wang, W.: An improved in situ and satellite SST analysis for climate, J. Climate, 15, 1609–1625, doi:10.1175/1520-0442(2002)015<1609:AIISAS>2.0.CO;2, 2002.

Roxy, K. M., Kapoor, R., Terray, P., Murtugudde, R., Ashok, K., and Goswami, B. N.: Drying of Indian subcontinent by rapid Indian Ocean warming and a weakening land-sea thermal gradient, Nat. Commun., 6, 7423, doi:10.1038/ncomms8423, 2015.

Saeed, F., Hagemann, S., and Jacob, D.: Impact of irrigation on the South Asian summer monsoon, Geophys. Res. Lett., 36, L20711, doi:10.1029/2009GL040625, 2009.

Saha, S. K., Halder, S., Kumar, K. K., and Goswami, B. N.: Pre-onset land surface processes and "internal" interannual variabilities of the Indian summer monsoon, Clim. Dynam., 36, 2077–2089, doi:10.1029/2011JD017291, 2011.

Saha, S. K., Halder, S., Rao, A. S., and Goswami, B. N.: Modulation of ISOs by land–atmosphere feedback and contribution to the interannual variability of Indian summer monsoon, J. Geophys. Res., 117, D1301, doi:10.1029/2011JD017291, 2012.

Sampaio, G., Nobre, C. A., Costa, M. H., Satyamurty, P., Soares-Filho, B. S., and Cardoso, M.: Regional climate change over eastern Amazonia caused by pasture and soybean cropland expansion, Geophy. Res. Let., 34, L17709, doi:10.1029/2007GL030612, 2007.

Seneviratne, S., Nicholls, N., Easterling, D., Goodess, C. M., Kanae, S., Kossin, J., Luo, Y., Marengo, J., McInnes, K., Rahimi, M., Reichstein, M., Sorteberg, A., Vera, C., and Zhang, X.: Changes in climate extremes and their impacts on the natural physical environment, in: SREX: Special Report on Managing the Risks of Extreme Events and Disasters to Advance Climate Change Adaptation, A Special Report of Working Groups I and II of the Intergovernmental Panel on Climate Change (IPCC), edited by: Field, C. B., Barros, V., Stocker, T. F., Qin, D., Dokken, D. J., Ebi, K. L., Mastrandrea, M. D., Mach, K. J., Plattner, G.-K., Allen, S. K., Tignor, M., and Midgley, P. M., Cambridge University Press, Cambridge, UK and New York, NY, USA, 109–230, 2012.

Sen Roy, S., Mahmood, R., Niyogi, D., Lei, M., Foster, S. A., Hubbard, K. G., Douglas, E. M., and Pielke Sr., R. A.: Impacts of the agricultural Green Revolution induced land use changes on air temperatures in India, J. Geophys. Res., 112, D21108, doi:10.1029/2007JD008834, 2007.

Sen Roy, S., Mahmood, R., Quintanar, A. I., and Gonzalez, A.: Impacts of irrigation on dry season precipitation in India, Theor. Appl. Climatol., 104, 193–207, doi:10.1007/s00704-010-0338-z, 2011.

Sheikh, M. M., Manzoor, N., Ashraf, J., Adnan, M., Collins, D., Hameed, S., Manton, M. J., Ahmed, A. U., Baidya, S. K., Borgaonkar, H. P., Islam, N., Jayasinghearachchi, D., Kothawale, D. R., Premalal, K. H. M. S., Revadekar, J. V., and Shrestha, M. L: Trends in extreme daily rainfall and temperature indices over South Asia, Int. J. Climatol., 35, 1625–1637, doi:10.1002/joc.4081, 2014.

Shkol'nik, I., Meleshko, V., Efimov, S., and Stafeeva, E.: Changes in climate extremes on the territory of Siberia by the middle of the 21st century: an ansemble forecast based on the MGO Regional Climate Model, Russ. Meteorol. Hydrol., 37, 71–84, 2012.

Singh, D., Tsiang, M., Rajaratnam, B., and Diffenbaugh, N. S.: Observed changes in extreme wet and dry spells during the South Asian summer monsoon season, Nat. Clim. Change, 4, 456–461, doi:10.1038/nclimate2208, 2014.

Snyder, P. K.: The influence of tropical deforestation on the Northern Hemisphere climate by atmospheric teleconnections, Earth Interact., 14, 1–32, doi:10.1175/2010EI280.1, 2010.

Solomon, S., Qin, D., Manning, M., Chen, Z., Marquis, M., Averyt, K. B., Tignor, M., and Miller, H. L. (Eds.): Climate Change 2007: The Physical Science Basis, Contribution of Working Group I to the Fourth Assessment Report of the Intergovernmental Panel on Climate Change, Cambridge University Press, New York, 996 pp., 2007.

Srinivasan, J. and Smith, G. L.: The role of heat fluxes and moist static energy in tropical convergence zones, Mon. Weather Rev., 124, 2089–2099, doi:10.1175/1520-0493(1996)124<2089:TROHFA>2.0.CO;2, 1996.

Srivastava, A. K., Rajeevan, M., and Kshirsagar, S. R.: Development of a high resolution daily gridded temperature data set (1969–2005) for the Indian region, Atmos. Sci. Lett., 10, 249–254, doi:10.1002/asl.232, 2009.

Stocker, T. F., Qin, D., Plattner, G.-K., Tignor, M., Allen, S. K., Boschung, J., Nauels, A., Xia, Y., Bex, V., and Midgley, P. M. (Eds.): IPCC, 2013: Climate Change 2013: The Physical Science Basis. Contribution of Working Group I to the Fifth Assessment Report of the Intergovernmental Panel on Climate

Change, Cambridge University Press, Cambridge, UK and New York, NY, USA, 1535 pp., 2013.

Stockli, R., Lawrence, D. M., Niu, G. Y., Oleson, K. W., Thornton, P. E., Yang, Z. L., Bonan, G. B., Denning, A. S., and Running, S. W.: Use of FLUXNET in the Community Land Model development, J. Geophys. Res., 113, G01025, doi:10.1029/2007JG000562, 2008.

Sud, Y., Shukla, J., and Mintz, Y.: Influence of land surface roughness on atmospheric circulation and precipitation: a sensitivity study with a general circulation model, J. Appl. Meteorol., 27, 1036–1054, doi:10.1175/1520-0450(1988)027<1036:IOLSRO>2.0.CO;2, 1998.

Takata, K., Saito, K., and Yasunari, T.: Changes in the Asian monsoon climate during 1700–1850 induced by preindustrial cultivation, P. Natl. Acad. Sci. USA, 106, 9586–9589, doi:10.1073/pnas.0807346106, 2009.

Tian, H., Banger, K., Bo, T., and Dadhwal, V. K.: History of land use in India during 1880–2010: large-scale land transfprmations reconstructed from satellite data and historical archives, Global Planet. Change, 121, 76–88, doi:10.1016/j.gloplacha.2014.07.005, 2014.

Tuinenburg, O. A., Hutjes, R. W. A., Jacobs, C. M. J., and Kabat, P.: Diagnosis of local land–atmosphere feedbacks in India, J. Climate, 24, 251–266, doi:10.1175/2010JCLI3779.1, 2011.

Wang, B., Ding, Q., and Joseph, P. V.: Objective definition of the Indian Summer Monsoon onset, J. Climate, 22, 3303–3316, doi:10.1175/2008JCLI2675.1, 2009.

Xavier, P. K., Marzin, C., and Goswami, B. N.: An objective definition of the Indian summer monsoon season and a new perspective on the ENSO-monsoon relationship, Q. J. Roy. Meteorol. Soc., 133, 749–764, doi:10.1002/qj.45, 2007.

Xue, Y., Janjic, Z., Dudhia, J., Vasic, R., and De Sales, F.: A review on regional dynamical downscaling on intraseasonal to seasonal simulation/prediction and major factors that affect downscaling ability, Atmos. Res., 147–148, 68–85, 2014.

Yatagai, A., Kamiguchi, K., Arakawa, O., Hamada, A., Yasutomi, N., and Kitoh, A.: APHRODITE: constructing a long-term daily gridded precipitation dataset for Asia based on a dense network of rain gauges, B. Am. Meteorol. Soc., 93, 1401–1415, doi:10.1175/BAMS-D-11-00122.1, 2012.

Zeng, X. and Beljaars, A.: A prognostic scheme of sea surface skin temperature for modeling and data assimilation, Geophys. Res. Lett., 32, L14605, doi:10.1029/2005GL023030, 2005.

Zeng, X., Shaikh, M., Dai, Y., Dickinson, R. E., and Myneni, R.: Coupling of the Common Land Model to the NCAR Community Climate Model, J. Climate, 15, 1832–1854, 2002.